VISCOUS-INVISCID FLOW INTERACTION IN STRATIFIED FLOW OVER A BARRIER

Thesis by

Tsung-chow Su

In Partial Fulfillment of the Requirements

For the Degree of

Aeronautical Engineer

California Institute of Technology

Pasadena, California

1973

(Submitted September 15, 1972)

ACKNOWLEDGMENTS

I would very much like to express my sincere gratitude and appreciation to Professor Lester Lees for bringing me this interesting problem and for both his technical and personal guidance during the course of this study. As teacher and advisor, his interest, encouragement and invaluable advice accompanied me throughout the course of my graduate work in GALCIT.

I would also like to express my gratitude to Professor Herbert B. Keller and Professor Theodore Y. T. Wu for their many helpful contributions and suggestions.

It is a most pleasant duty for me to express my sincere appreciation and thanks to Professor Toshi Kubota for his kind help, invaluable advice and stimulating discussions.

I wish to acknowledge the receipt of financial support from the California Institute of Technology (1969 ~1972). The work discussed in this thesis was carried out under the sponsorship and with the financial support of the Air Force of Scientific Research under Grant No. AFOSR-68-1399.

This thesis is dedicated to my parents.

ABSTRACT

The gross effect of boundary layer separation on the flow field of stratified flow over a barrier was studied by means of the integral method of Lees and Reeves.

The complete integral formulation of both inner and outer flow field of stratified flow over a barrier was obtained.

Furthermore, an iteration scheme of computation is proposed for the simple case of incompressible homogeneous flow over a barrier with viscous-inviscid interaction included.

However, in viewing the increasing importance, a considerable amount of work remains to be done on this problem.

TABLE OF CONTENTS

Table of Contents (Continued)

LIST OF FIGURES

LIST OF SYMBOLS

a_o effective origin of Blasius boundary layer

N^{C_j} $\dfrac{N!}{(N-j)!\ j!}$

C_f local skin-friction coefficient, $\tau_w / \frac{1}{2} \rho_o U_o^2$

C_D $\dfrac{2}{\rho_o U_e^3} \int_o^\infty \tau \dfrac{\partial u}{\partial y}\, dy$

f Horizontal velocity in strong interaction region, computed from boundary layer equation

f nondimensional stream function

$f'(\eta)$ U/U_e, similar velocity profile

$f_2(x)$ $f(x)-u_1(x)$

$\hat{f}_2(\xi)$ $f_2[x(\xi)]$, $\xi = (x-x_J)^{\frac{1}{2}}$

g gravity acceleration

$g(x)$ slope of effective body in weak interaction region, computed from boundary layer equation

g_1

g_2 g_1, g_2 are constant, obtained from $g(x_J)=\hat{g}(x_J)$, $g'(x_J)=\hat{g}'(x_J)$

$\hat{g}(x)$ $\dfrac{g_1}{x} + \dfrac{g_2}{x^2}$

$\bar{g}_2$ $g_2 + \hat{g}_2$

$\hat{g}_2$ $x_J \int_o^{x_J} g(x)dx$

H velocity profile shape factor θ/δ^*

$H(\psi)$ Bernoulli's function $= \dfrac{q^2}{2} + \dfrac{P}{\rho} + gy$

H_o H at leading edge

List of Symbols (Continued)

H_2	$\frac{1}{2} \frac{d^2H}{ds^2}$ at leading edge
H_b	shape factor for Blasius velocity profile
J	θ^*/δ^*
J_o	J at leading edge
$J_n(x)$	Bessel function of the first kind
$K(x, \xi)$	kernel used in stratified flow calculation (4, 20)
ℓ	characteristic length of the barrier
L	Lighthill's correction factor
n	coordinate axis normal to the wall of the barrier
P	Pressure or Integral quantity defined as $\frac{\delta^*}{u_e} (\frac{\partial u}{\partial n})_w$
P_o	reference pressure or $\frac{\delta^*}{u_e} (\frac{\partial u}{\partial n})_w$ at leading edge
$\underline{q}$	velocity vector
r	$(x^2+y^2)^{\frac{1}{2}}$
$\bar{R}$	Radius of curvature
R	$\frac{2\,\delta^*}{u_e^2} \int_o^\delta (\frac{\partial u}{\partial n})^2 dn$
R_i	Richardson No. $\equiv g \left\lvert \frac{1}{\rho} \frac{d\rho}{dy_o} \right\rvert \epsilon_b^2/U_o^2$
s	distance measured along the wall of the barrier
s_J	s at joining point for numerical iteration
t	time
u	velocity component in x-direction
u_1	$\frac{du_e}{ds}$ at leading edge or x-velocity in problem 1

List of Symbols (Continued)

u_2	x-velocity for $x < x_J$ in problem 2
$\underset{\sim}{u}$	velocity vector
U_o	characteristic velocity
U_e	surface velocity at the edge of effective body
u_3	$\frac{1}{6} \frac{d^3 u_e}{ds^3}$ at leading edge
v	y-velocity or slope of effective body
v_2	slope of effective body in problem 2
w	complex velocity $u - iv$
x	horizontal axis of Cartesian coordinate
x_J	position of joining point in iteration
x_M	the farthest computed point from origin
y	coordinate axis normal to x
y_o	elevation of streamline at far upstream
y_e	the height of effective body
y_b	the barrier height
Y_n	Bessel function of the second kind
Z	$x + iy$
δ_o	$\delta^{*\frac{1}{2}}$ at leading edge
δ_2	$\frac{1}{2} \frac{d\delta^{*2}}{ds}$ at leading edge
δ	boundary layer thickness
δ^*	displacement thickness
Δ	streamline displacement
ϵ_b	characteristic barrier height
ϵ_v	$\frac{\nu}{U_o \ell}$

I. INTRODUCTION

The study of stratified flow over barriers has been limited to linearization of Euler equation for a number of years. It was not until 1953 Long (1) showed that, for the special case in which both the dynamic pressure and the vertical density gradient far upstream of the barrier are constant, the full equations of steady, two-dimensional inviscid flow could be transformed to Helmholtz's equation, a linear one. This equation together with appropriate boundary conditions, i.e., zero normal velocity on barriers and no waves far upstream, represents a well-posed linear boundary-value problem, which has served as the basis of extensive analyses of flow over a barrier of finite size.

Although theoretical investigation of stratified flow over barriers is extensive, very little experimental work, with which the theories may be compared, has been conducted. It was shown by Davis (2) that the discrepancy between Long's theory and experiment, which is often very great, is associated with the generation of intense turbulence behind the barrier. It is obvious that Long's inviscid model is invalid if and when boundary-layer separation occurs.

Objective for the present research is to carry out an analysis of stratified flow over a barrier in the two-dimensional half plane, with emphasis on the change of flow field due to boundary layer separation. Unlike usual problems of aeronautics, in those problems of atmospheric and environmental fluid mechanics, e.g., stratified flow over a barrier, one is mainly interested in the outer region of the flow field.

Although inviscid theory gives a reasonably good approximation for this region, viscosity plays a major role in determining the boundary condition if and when boundary layer separation occurs, and inviscid theory by itself becomes no longer applicable. This leads us to the study of flow separation by simultaneous treatment of inviscid and viscous flow field.

The difficulty inherent in the separated flow problem is that the static pressure distribution cannot be specified a priori, but is determined by the interaction between the outer inviscid flow and the inner viscous layer near the surface. Hence, in order to develop a complete theoretical model for the problem of stratified flow over barriers with boundary layer separation, one needs to be able to calculate both the boundary layer and inviscid flow field and then to couple the two properly. In recent years, the versatility of moment or integral method for treating laminar or turbulent viscous-inviscid interactions at supersonic speeds has been amply demonstrated (Lees and Reeves (3), Alber(4), Klineberg(5), Grange(5)). It is only natural to ask whether or not the method developed for supersonic flow can be extended and applied to the problem of low speed flow. Although the elliptic nature of low speed flow problem makes the problem much more difficult and requires that the interaction between the inviscid flow and the viscous flow is global, while in supersonic two-dimensional flow it may be approximated by local interaction.

For simplicity, only slender barrier problem is considered. The flow in the inner viscous layer is assumed to be governed by the boundary layer equations; i.e., the streamwise gradient is much

smaller than the transverse gradient of the same quantity. An important difference from the conventional boundary layer theory is that even in the first approximation the pressure distribution is given by the inviscid flow theory, not with zero boundary layer thickness, but with the displacement effect of the boundary layer included.

The boundary layer flow is solved approximately by adopting the integral method developed by Lees, Reeves and Klineberg (3, 5).

The outer inviscid flow solution is expressed in terms of an integral of flow due to distributed doublet with strength related to the effective shape of barrier.

II. DESCRIPTION OF THE STRATIFIED FLOW FIELD

The principal object of this study is to estimate the gross effect of boundary layer separation on the stratified flow field. In order to formulate a simple model for stratified flow over a barrier, it is most necessary to make use of the available experimental results so as to delineate, if possible, the most important features of a highly complex flow pattern.

II. 1. The Two-Dimensional Stratified Flow Field

Several important regions in the flow field of stratified flow over a barrier have been clearly established by the investigation of Long (1, 6, 7), Pao (8, 9, 10, 11), Davis (2), and many others. By the use of fine aluminum powders as tracers, several distinct features of stable stratified flow field are observed experimentally with flow visualization techniques, (2, 7, 8). With the experimental results of the above authors, it is possible to discern certain distinct features of the flow field of stratified fluid over a barrier.

II. 2. Lee Waves and Boundary-Layer Separation

One of the most interesting phenomenon on the flow field of stratified flow over a barrier is the formation of the lee waves, or waves in the lee of the barriers, which are similar to atmospheric waves in the lee of mountain ranges.

To see how these waves can arise in a stratified fluid, one could consider the vorticity equation for an incompressible stratified fluid:

$$\frac{D\underset{\sim}{\omega}}{Dt} + \nu \nabla \times (\nabla \times \underset{\sim}{\omega}) = (\underset{\sim}{\omega} \cdot \nabla)\underset{\sim}{u} + \rho^{-2} \nabla\rho \times \nabla P$$

Rate of change of vorticity following a moving fluid parcel	Viscous diffusion of vorticity	Generation of vorticity by stretching	Generation of vorticity by stratification

where ν is the kinematic viscosity and is assumed to be a constant for the present problem.

The term $\rho^{-2}\nabla\rho\times\nabla P$ shows that the vorticity can be generated through interaction of the density and pressure gradient; it is a new mechanism for generating vorticity introduced by stratification.

As the fluid descends in the lee of the barrier, the last term in the vorticity equation, $\rho^{-2}\nabla\rho\times\nabla P$, produces a vorticity in a counterclockwise sense. This rotation induces the descending fluid to turn upward. On the way up, vorticity of opposite sense is generated and turns the fluid down again. Thus, lee wave is generated behind the barrier (see figure 1) if the flow is stably stratified.

Under the first crest of the lee wave, there exists an area corresponding to a minimum of velocity, which is obvious (figure 1) from the conservation of mass flux between streamlines in two-dimensional flow, and therefore a region of maximum dynamic pressure. The adverse pressure gradient produced near upstream of this region, if intense enough, will cause the boundary layer separation. The fluid in the boundary layer is then carried into separated-flow region to form a large turbulent eddy. It is likely that this turbulent eddy, due partly to boundary layer separation and partly to overturning

instability, could dissipate so much energy, which would otherwise go into wave motion, that the lee waves further downstream are greatly weakened. This effect, which has evidently been shown by comparing the theoretical prediction and experimental result performed by Davis, has a profound effect on stratified flow field and is the main object of the present study.

II. 3. The Phenomenon of Blocking

The upstream blocking effect which slows down the flow in front of the barrier is shown in Figure 2. This phenomenon of stratified flow has been the subject of several recent papers. All the experimental studies of Long (7), Debler (12) and Yih (13) indicate that at very large Richardson numbers, stagnation zones occur upstream of the barriers. Trustrum (14) investigated the initial value problem corresponding to Long's model and suggested that the final state may involve waves upstream. Bretherton (15) solved the initial value problem for the limit of infinite Richardson number and found that at the upstream of the barrier, there exists a blocked region of stagnant fluid which is separated from the main flow by a thin shear layer. Kao (16) assumed that such blocked regions exist and calculated flows over barriers using an ad hoc modification of Long's model.

The present study is mainly concerned with stratified flow over slender barriers with boundary-layer separation. In order to have boundary-layer separation occur in the flow over a slender barrier, the flow field with relatively high characteristic velocity is considered. If characteristic velocity is U_o, characteristic barrier height is ϵ_b,

Richardson number, $g\left|\frac{1}{\rho}\frac{d\rho}{dy_0}\right|\epsilon_b^2/U_0^2$, should be small for the slender barrier. Since upstream blocking effect is small if Richardson number is not very large, it is likely that the blocking effect is negligible for the case of a slender barrier. Davis' experiment shows that, for Richardson number between 4.0 to 5.0, the effects of upstream blocking, if it occurs, are insignificant compared with the other differences between theory and experiment, such as the boundary layer separation[2]. The computation of Kao's work mentioned above, which indicates that depth of stagnant zone decreases as Richardson number decrease, also seems to confirm this argument.

For the case of bluff body, since boundary layer separation may take place even for flow with large Richardson number, the blocking effect should be taken into account.

With above understanding about upstream blocking effect in mind, and because a simple stratified flow model is sought in order to bring out the essential features of the viscous-inviscid interaction, the blocking effect is neglected for "slender" barrier problem.

II. 4. The Turbulent Rotor

The turbulent rotor is an isolated turbulent region which forms in the trough of a lee wave but away from the barrier (see figure 3). This phenomenon is relevant to the mountain wave turbulence and its occurrence is associated with strong stratification, or more precisely, with large Richardson numbers. These turbulent eddies have strong interaction with mean flow field and remove so much energy that it caused some discrepancy between theory and experiment (7).

Since Richardson numbers associated with the slender barrier of the present study are not very large, the occurrence of the turbulent rotor is unlikely and hence its effect is rightly neglected.

II. 5. Flow Field of Stratified Flow over a "Slender" Barrier

All of the features noted above have been found in experiments for stratified flow over a barrier. However, in the present study of a slender barrier with boundary-layer separation, the phenomenon of blocking and the turbulent rotor is negligible. Only the essential feature of lee wave and boundary-layer separation are retained, which is relevant to the case that Richardson number is small or to the turbulence behind mountains with weakly stratified wind.

III. FORMULATION OF INNER VISCOUS LAYER

Very close to the wall there appears to be a region where the fluid motion is still predominantly viscous, and the velocity rises steeply. This is called inner viscous layer, or boundary-layer.

III. 1. Formulation of Laminar Viscous Layer

In the analysis of inner viscous layer, a curvilinear orthogonal system of co-ordinates is introduced in which s-axis is in the direction of the wall, the n-axis being perpendicular to it as Figure 4. The corresponding velocity components are denoted by u and v and the radius of curvature of barrier at a point s is denoted by $\bar{R}(s)$, being positive when the wall is convex outward and negative otherwise.

In this co-ordinate system the Navier-Stokes equations for steady two-dimensional flows are:

$$\frac{\bar{R}}{\bar{R}+n}u\frac{\partial u}{\partial s}+v\frac{\partial u}{\partial n}+\frac{uv}{\bar{R}+n}=-\frac{\bar{R}}{\bar{R}+n}\frac{1}{\rho}\frac{\partial P}{\partial s}+\nu\left[\frac{\bar{R}^2}{(\bar{R}+n)^2}\frac{\partial^2 u}{\partial s^2}+\frac{\partial^2 u}{\partial n^2}+\frac{1}{\bar{R}+n}\frac{\partial u}{\partial n}-\frac{u}{(\bar{R}+n)^2}+\frac{2\bar{R}}{(\bar{R}+n)^2}\frac{\partial v}{\partial s}-\frac{\bar{R}}{(\bar{R}+n)^3}\frac{d\bar{R}}{ds}v+\frac{\bar{R}n}{(\bar{R}+n)^3}\frac{d\bar{R}}{ds}\frac{\partial u}{\partial s}\right]-g\sin\theta_B \tag{3.1}$$

$$\frac{\bar{R}}{\bar{R}+n}u\frac{\partial v}{\partial s}+v\frac{\partial v}{\partial n}-\frac{u^2}{\bar{R}+n}=-\frac{1}{\rho}\frac{\partial P}{\partial n}+\nu\left[\frac{\partial^2 v}{\partial n^2}-\frac{2\bar{R}}{(\bar{R}+n)^2}\frac{\partial u}{\partial s}+\frac{1}{\bar{R}+n}\frac{\partial v}{\partial n}+\frac{\bar{R}^2}{(\bar{R}+n)^2}\frac{\partial^2 v}{\partial s^2}-\frac{v}{(\bar{R}+n)^2}+\frac{\bar{R}}{(\bar{R}+n)^3}\frac{d\bar{R}}{ds}u+\frac{\bar{R}n}{(\bar{R}+n)^3}\frac{d\bar{R}}{ds}\frac{\partial v}{\partial s}\right]-g\cos\theta_B \tag{3.2}$$

$$\frac{\bar{R}}{\bar{R}+n}\frac{\partial u}{\partial s}+\frac{\partial v}{\partial n}+\frac{v}{\bar{R}+n}=0 \tag{3.3}$$

The inner viscous layer is assumed to be governed by the boundary-layer equations; i. e., the streamwise gradient is much smaller than the transverse gradient of the same quantity. In the present study, only slender barrier is treated, so that it is natural to assume that boundary-layer thickness is small compared with radius of curvature of the barrier's wall. With the above assumptions in mind and for the case when no large variations in curvature occur, i. e., $\frac{dR}{ds} \sim O(1)$, the complete Navier-Stokes equation could be reduced to

$$u\frac{\partial u}{\partial s} + v\frac{\partial u}{\partial n} = -\frac{1}{\rho}\frac{dP}{ds} - \nu\frac{\partial^2 u}{\partial n^2} - g\sin\theta_B \qquad (3.4)$$

$$\frac{\partial u}{\partial s} + \frac{\partial v}{\partial n} = 0 \qquad (3.5)$$

where the second equation (3.2) becomes $\frac{1}{\rho}\frac{\partial P}{\partial n} = \frac{u^2}{R} - g\cos\theta_B$. Thus the pressure gradient in the perpendicular direction is now of order one. The pressure difference between wall and outer edge of the boundary-layer is now of order δ . So that in the case of a curved wall, the pressure P in the boundary-layer is assumed to be constant. In (3.4) the $\frac{dP}{ds}$ term could then be related to outer inviscid flow field by Bernoulli's equation.

The Bernoulli's equation for steady, non-diffusive inviscid stratified flow could be obtained as follows

Governing Euler Equation

$$(\vec{q}\cdot\nabla)\vec{q} = -\frac{1}{\rho}\nabla P + \nabla(-gy) \qquad (3.6)$$

By vector identity, (3.6) implies

$$\nabla\left(\frac{q^2}{2}\right)-\vec{q}\times(\nabla\times\vec{q})=-\frac{1}{\rho}\nabla P+\nabla(-gy) \tag{3.7}$$

Scalar product of (3.7) and $\vec{q}$ yields

$$\vec{q}\cdot\nabla\left(\frac{q^2}{2}\right)=-\vec{q}\cdot\left(\frac{1}{\rho}\nabla P\right)+\vec{q}\cdot\nabla(-gy)$$

$$=-\vec{q}\cdot\left(\nabla\frac{P}{\rho}-P\nabla\frac{1}{\rho}\right)+\vec{q}\cdot\nabla(-gy) \tag{3.8}$$

For a non-diffusive fluid $\vec{q}\cdot\nabla\rho=0$

$$\therefore\quad \vec{q}\cdot P\nabla\left(\frac{1}{\rho}\right)=\frac{P}{\rho^2}\vec{q}\cdot\nabla\rho=0$$

Hence, (3.8) becomes

$$\vec{q}\cdot\quad\nabla\ \left(\frac{q^2}{2}+\frac{P}{\rho}+gy\right)=0 \tag{3.9}$$

which implies

$$\frac{q^2}{2}+\frac{P}{\rho}+gy=H(\psi)$$

where $H(\psi)$ is a function of the stream function ψ and could be evaluated from the far-upstream condition. Thus (3.9) becomes

$$\frac{1}{2}(u^2+v^2)+\frac{P}{\rho}+gy=\frac{U_{-\infty}^2}{2}+\frac{P_{-\infty}}{\rho_{-\infty}}+gy_0 \tag{3.10}$$

where $y_0\ (\psi)$ is the height of streamline ψ = constant in the far upstream.

Consistent with Long's model, the far-upstream conditions for the present study are:

$$\rho_{-\infty} U_{-\infty}^2 = \alpha \quad , \quad \frac{d\rho}{dy_o} = \beta \tag{3.11}$$

$$\rho_{-\infty} = \rho_o - \beta y_o \qquad U_{-\infty}^2 = \frac{\alpha}{\rho_o - \beta y_o} \tag{3.12}$$

static pressure $P_{-\infty}$ could be calculated by $\frac{dP_{-\infty}}{dy_o} = -\rho_{-\infty} g$

or $$\frac{dP_{-\infty}}{dy_o} = -(\rho_o - \beta y_o) g$$

$$\therefore \quad P_{-\infty} = -\rho_o g y_o + \frac{y_o^2}{2} \beta g + P_o \quad . \tag{3.13}$$

Substituting (3.12), (3.13) into (3.10), we obtain

$$\frac{1}{2}(u^2 + v^2) + \frac{P}{\rho_o - \beta y_o} + g y = \frac{\frac{\alpha}{2} - \frac{y_o^2}{2}\beta g + P_o}{\rho_o - \beta y_o} \tag{3.14}$$

at the edge of boundary layer

$$y = y_b + \delta \cos\theta_B \doteq y_b$$

Furthermore $\beta y_o \propto \frac{d\rho}{dy_o} \cdot \delta \ll \rho_o$ and $v_e \ll u_e$.

Therefore (3.14) becomes

$$\frac{1}{2} U_e^2 + \frac{P}{\rho_o} + g y_b = \frac{\alpha}{2\rho_o} + \frac{P_o}{\rho_o} + O\left(\frac{\delta}{L}\right) \tag{3.15}$$

Differentiating (3.15) with respect to s , one obtains

$$U_e \frac{dU_e}{ds} + \frac{1}{\rho_o} \frac{dP}{ds} + g \frac{dy_b}{ds} = 0 \tag{3.16}$$

Substituting (3.16) into (3.4), one obtains

$$\rho\left(u\frac{\partial u}{\partial s}+v\frac{\partial u}{\partial n}\right)=\rho_0 U_e\frac{dU_e}{ds}+\mu\frac{\partial^2 u}{\partial n^2}+\rho_0 g\frac{dy_b}{ds}-\rho g\sin\theta_B$$

Since $\frac{dy_b}{ds}\equiv\sin\theta_B$, the above equation becomes

$$\rho\left(u\frac{\partial u}{\partial s}+v\frac{\partial u}{\partial n}\right)=\rho_0 U_e\frac{dU_e}{ds}+\mu\frac{\partial^2 u}{\partial n^2}+(\rho_0-\rho)g\sin\theta_B \qquad (3.17)$$

Since

$$\rho=\rho_0-\beta y_0=\rho_0+O(\delta^*)\ ,$$

consistent with boundary-layer theory (or approximation) $\rho\doteq\rho_0$ inside boundary layer, (3.17) becomes

$$u\frac{\partial u}{\partial s}+v\frac{\partial u}{\partial n}=U_e\frac{dU_e}{ds}+\nu_0\frac{\partial^2 u}{\partial n^2} \qquad (3.18)$$

$$\frac{\partial u}{\partial s}+\frac{\partial v}{\partial n}=0 \qquad (3.5)$$

Thus the governing equations of the inner viscous layer are given in (3.18) (3.5), provided the pressure distribution term $U_e\frac{dU_e}{ds}$ is given correctly by an inviscid theory with the displacement effect of the boundary-layer included.

In order to bring out the essential features of the complex interaction phenomenon, integral form of governing conservation equations are used, namely, momentum integral equation and

mechanical energy equation, in the inner viscous layer.

Using the continuity equation (3.5), the momentum equation (3.18) is integrated across the boundary layer to obtain the integral momentum equation

$$H\frac{d\delta^*}{ds} + \delta^*\frac{dH}{ds} + (2H+1)\frac{\delta^*}{U_e}\frac{dU_e}{ds} = \frac{\nu_0 P}{U_e \delta^*} \tag{3.19}$$

where $\delta^* = \int_0^\delta (1-\frac{u}{U_e})\,dn$, $\theta = \int_0^\delta \frac{u}{U_e}(1-\frac{u}{U_e})\,dn$

$$P = \frac{\delta^*}{U_e}\left(\frac{\partial u}{\partial n}\right)_w \quad , \quad H = \frac{\theta}{\delta^*}$$

Multiplying momentum equation (3.18) by u and integrating across the boundary layer, we obtain the integral mechanical energy equation

$$J\frac{d\delta^*}{ds} + \delta^*\frac{dJ}{ds} + 3J\frac{\delta^*}{U_e}\frac{dU_e}{ds} = \frac{\nu_0 R}{U_e \delta^*} \tag{3.20}$$

where $J = \theta^*/\delta^*$

$$\theta^* = \int_0^\delta \frac{u}{U_e}\left(1-\frac{u^2}{U_e^2}\right)dn \quad , \quad R = \frac{2\delta^*}{U_e^2}\int_0^\delta \left(\frac{\partial u}{\partial n}\right)^2 dn$$

From the continuity equation $\left(\frac{v}{u}\right)_{inv.} = y_b' + \frac{d\delta^*}{ds}$, through which the boundary layer and the inviscid flow field were coupled. The details of the coupling will be discussed in the next section.

The integral approach devised by Lees and Reeves (3) has demonstrated that the over-all character of the viscous inviscid interaction can be sufficiently described provided that the velocity profiles, from which integral quantities are derived, has the correct qualitative behavior. The recent work of Alber (4), Lees and Alber (17) further confirm this statement. In the present study, the integral properties for laminar separating and reattaching flow were generated by Stewartson's (18) "lower branch" solution of Falkner-Skan equations.

$$f''' + ff'' + \bar{\beta}(1 - f'^2) = 0$$

with the boundary conditions

$$f(0) = f'(0) = 0 \quad ; \quad f'(\infty) = 1 \qquad \frac{u}{u_e} = f'(\eta)$$

For a given value of the form factor H, there exists each a corresponding value of the non-dimensional integral quantities J, R and P. These quantities are then curve fitted as a function of H to facilitate differentiation and numerical integration. The functions are the following (see figure 5).

for 0.47847 ≥ H ≥ 0.12127 :

	H^o	H	H^2	H^3	H^4	H^5
J	0.04646407	1.193432	0.3331707	0.859477		
R	4.192635	−22.01915	62.30798	−124.5095	185.8661	−122.2053
P	−0.6719037	−3.418973	54.70549	−180.8112	288.6487	−185.6851

for 0.12127 ≥ H ≥ 0.07856 :

	H^o	H	H^2	H^3	H^4	H^5
J	0.04647407	1.193432	0.3331707	0.859477		
R	4.192635	−22.01915	62.30798	−124.5095	185.8661	−122.2053
P	-0.6918802	0.7872477	-118.7278	2505.601	-17608.7	43287.775

for 0.07856 ≥ H ≥ 0.04313 :

	H^o	H	H^2	H^3	H^4	H^5
J	0.04647407	1.193432	0.3331707	0.859477		
R	5.000497	52.79329	452.0378	−1751.461		
P	−0.6918802	0.7872477	−118.7278	2505.601	−17608.7	43287.775

for $0.04313 \geqslant H \geqslant 0.01992$:

	H^o	H	H^2	H^3	H^4	H^5
J	0.01736142	4.766541	−199.261	597.863	91809.25	
R	5.000497	−52.79329	452.0378	−1751.461		
P	−0.1907012	−68.05284	4145.418	−134465.3	2164912.0	−13540630.0

for $0.01992 \geqslant H \geqslant 0.00048$

	H^o	H	H^2	H^3	H^4	H^5
J	0.01736142	4.766541	−199.261	5987.863	91809.25	
R	8.468969	−575.1523	26674.89	−440554.6		
P	−0.1907012	−68.05284	4145.418	−134465.3	2164912.0	−13540630.0

Since P, R, J are known functions of H , (3.19) (3.20) give two equations for three unknowns, and one more equation which is given by the inviscid theory and coupled with the viscous region through continuity equation will be discussed later, thus complete the formulation.

III. 2. Formulation of Turbulent Boundary Layer

When the density stratified flow passes a slender barrier with blunt nose, the clockwise free stream vorticity generated by the density stratification tends to destabilize the boundary-layer at the forward portion of the barrier and lee wave (see Figure 6). Hence the boundary-layer is likely to be fully turbulent for most part of the flow, and the laminar case treated in III. 1. can be considered only as an introductory section to the formulation of turbulent boundary-layer.

For the laminar layer, if the radius of curvature of the surface is much larger than the boundary layer thickness, the curvature effect, arising from the kinematics of curved flow and the curvature of mean flow streamlines, is less important for the calculation of boundary viscous layer. Van Dyke (19) has shown that the effects of the additional curvature of the mean flow streamlines are of the second order smallness.

Although the curvature effect could be well neglected for the calculation of laminar boundary-layer, it is believed that the turbulent flows are very sensitive to the curvature of the mean flow streamlines.

The wall curvature influences the turbulent flow in a manner which unfortunately is not yet known. For the present study, it seems likely that we could neglect the curvature effect not just for simplicity, but also for the following reasons.

The first reason is related to the slender body approximation. For the thin barriers, the curvature should be vanishingly small all the way along barriers except near the blunt leading edge. So it seems that the curvature influence, if it exists, should still be small for the major portion of the barriers.

Recent experimental investigation of So and Mellor (20) on turbulent boundary-layers along a curved surface indicates that on the convex surfaces the intensities of turbulence are decreased and the ability of the flow to support adverse pressure gradient is reduced, while the concave curvature tends to promote mixing in the turbulent boundary layer. On the other hand, at the forward portion of the barrier or lee wave, the clockwise free stream vorticity generated by density stratification tends to create the point of inflection in the horizontal velocity profile. This will either promote transition or turbulent mixing in the boundary layer. At the lee of the barrier or lee wave, the counter-clockwise free stream vorticity generated by stratification tends to wash out the point of inflection in the horizonal velocity profile and will either delay the transition or reduce turbulent mixing in the boundary layer. It will also increase the ability of the flow for supporting adverse pressure gradient.

Thus, the second reason to neglect the curvature effect in the turbulent boundary layer of the present study is that the curvature effect produced by the additional curvature of the mean flow streamline tends to compensate the effect of free stream vorticity generated by density stratification of outer inviscid flow.

With the above discussion in mind, it seems possible to neglect both free stream vorticity effect and curvature effect in order to get a gross feature of the flow field, at least for the study of slender body.

Next question which naturally arises is in regard to the effect of density inhomogeneity on the turbulent bounday-layer. Does the approximation, $\rho \doteq \rho_0$, which has been shown for the case of laminar boundary layer, still hold true for the general case of turbulent boundary layer?

In order to answer this question, let us point out that the vorticity generated by stratification is of the order of the Brunt-Väisälä frequency, i. e., $\left(\frac{1}{\rho_0}\frac{d\rho}{dy_0}g\right)^{1/2}$. On the other hand, the frequency of the largest turbulent eddies is of the order of U_0/ϵ_b , the frequency of smaller eddies is even higher. In the present study of a slender barrier, Richardson number, $\frac{\epsilon_b^2}{U_0^2}\left(\frac{1}{\rho_0}\frac{d\rho}{dy_0}g\right)$, is small compared to one, which implies that $\frac{U_0}{\epsilon_b} > \left(\frac{1}{\rho_0}\frac{d\rho}{dy_0}g\right)^{1/2}$. The measure of time scale in stratified flow is reciprocal of Brunt-Väisälä frequency, which means to any forcing of fluid with a frequency greater than Brunt-Väisälä frequency the fluid acts as a homogenous fluid.

Because frequency of turbulent motion is greater than that of stratification, the fluid could still be considered as homogenous fluid. Inside the turbulent boundary-layer, following a similar

argument as the laminar case, ρ could be approximately equal to ρ_0 consistent with boundary-layer approximation.

With the above discussion in mind, except for the length scale introduced into the problem through the viscous dissipation integral $\int_0^\delta \tau \frac{\partial u}{\partial y} dy$ the turbulent case is not very much different from the laminar case discussed before. One could then obtain integral momentum equation and mechanical energy equation for turbulent boundary -layer, following some integral technique adopted in the previous sections.

Integral momentum equation

$$H \frac{d\delta^*}{ds} + \delta^* \frac{dH}{ds} + (2H+1) \frac{\delta^*}{U_e} \frac{dU_e}{ds} = \frac{C_f}{2} \tag{3.21}$$

Integral mechanical energy equation

$$J \frac{d\delta^*}{ds} + \delta^* \frac{dJ}{ds} + 3J \frac{\delta^*}{U_e} \frac{dU_e}{ds} = C_D$$

$$C_D \equiv \frac{2}{\rho_0 U_e^3} \int_0^\infty \tau \frac{\partial u}{\partial y} dy \tag{3.22}$$

The continuity equation is again simply $\left(\frac{v}{u}\right)_{inv.} = y_b' + \frac{d\delta^*}{ds}$ through which inner and outer region were coupled.

In order to construct an integral method for the reverse flow region, we use recently developed Alber's model of the turbulent shear stress in the separated flow region [22]. Alber also obtained a family of reverse flow velocity profiles by integration of the turbulent

Falkner-Skan equations for the turbulent counterpart of the Stewartson lower-branch laminar reverse flow[22]. By using this family of velocity profiles, shear work integral C_D and the mechanical energy shape factor J can be expressed as functions of shape factor H. Comparison of theoretical velocity profiles with transonic duct data (23) shows good agreement.

By following the same integral approach as in the laminar case and using the integral curves mentioned above, these integral quantities are then curve-fitted as function of H to facilitate numerical work.

IV. FORMULATION OF INVISCID OUTER FLOW FIELD

In order to calculate the inviscid flow field of stratified flow over a slender barrier with the displacement effect of boundary layer included, the solution derived for thin airfoil theory was used.

In the present study the flow field is assumed to be two-dimensional and of infinite extent.

IV.1. Flow with Zero Density Gradient; Potential Flow Case

For the case of potential flow the well known solution derived for thin airfoil theory was used (Fig. 8).

$$\frac{"U_e"}{U_o} = 1 + \frac{1}{\pi}\int_{-\infty}^{\infty} \frac{\tan \Theta(\xi)}{x - \xi}\, d\xi \qquad (4.1)$$

Where "U_e" is surface velocity calculated by linear theory, it is not valid at leading edge and remains to be corrected later.

From Figure 8 it is obvious that

$$\Theta(x) \doteqdot \theta_B(x_1) + \tan^{-1}\left(\frac{d\delta^*(x_1)}{ds}\right) \qquad (4.2)$$

and $$x_1 - x = \delta^*(x_1)\sin\theta_B(x_1) \qquad (4.3)$$

Since the boundary layer is thin, $x_1 - x$ is small, and we could approximate $\Theta(x_1)$ by expanding Θ into Taylor series around $x_1 = x$ in order to evaluate $\Theta(x)$

$$\Theta(x_1) = \Theta(x) + \frac{d\Theta(x)}{ds}(x_1 - x) + \cdots \doteqdot \Theta(x) \qquad (4.4)$$

Comparison of (4.2) and (4.4) implies

$$\Theta(x_1) = \theta_B(x_1) + \tan^{-1}\left(\frac{d\delta^*(x_1)}{ds}\right) \qquad (4.5)$$

where $x_1 \geq 0$ from figure (8). We could rewrite (4.5) as

$$\Theta(x) = \theta_B(x) + \tan^{-1}\left(\frac{d\delta^*}{ds}(x)\right) \quad \text{for } x > 0 \tag{4.6}$$

which implies

$$\tan\Theta(x) \doteq y_b'(x) + \delta_s^*(x) \qquad x>0 \qquad O(y_b'\delta_s^*) \ll 1$$

where $$y_b'(x) \equiv \tan\theta_B(x) \;, \quad \delta_s^* \equiv \frac{d\delta^*}{ds} \tag{4.7}$$

The difference between x and x_1 is neglected in the present analysis, because the boundary layer is very thin near the leading edge and elsewhere the slope of the barrier contour is very small.

Since slender body assumption is violated near the blunt leading edge, in the present study Lighthill's correction is brought in to obtain a uniformly valid expression of velocity distribution at the surface of the effective body, the body which includes the effect of displacement of boundary layer.

Near the leading edge of Joukowski barrier, locally it is a parabola. The exact surface speed on the parabola is easily calculated as $q = U_i\left(\frac{s^*}{s^*+R_o/2}\right)^{1/2}$, where U_i is the maximum speed on parabola, s^* is horizontal distance from the effective leading edge, R_o nose radius. On the other hand thin airfoil theory gives the solution of "U_e" = U_i.

It is now claimed that the ratio of these two expressions serves as a multiplicative correction factor that converts the formal thin airfoil solution "U_e" for the speed on any "airfoil" of nose radius R_o into a uniformly valid approximation U_e

$$U_e = \left(\frac{S^*}{S^* + R_0/2}\right)^{1/2} \text{“}U_e\text{”} \tag{4.8}$$

This rule was first deduced by Lighthill (1951) and hence is referred to as Lighthill's rule.

From (4.1) and (4.8) we obtain corrected surface speed

$$\frac{U_e(x)}{U_0} = \left(\frac{S^*}{S^* + R_0/2}\right)^{1/2} \left[1 + \frac{1}{\pi}\int_{-\infty}^{\infty} \tan\Theta(\xi) \frac{d\xi}{x-\xi}\right] \tag{4.9}$$

From the expression of $\tan\Theta$ given in (4.6) and (4.7) we obtain:

$$\frac{1}{\pi}\int_{-\infty}^{\infty} \tan\Theta(\xi) \frac{d\xi}{x-\xi} = \frac{1}{\pi}\int_0^{\infty} y_b'(\xi) \frac{d\xi}{x-\xi} + \frac{1}{\pi}\int_0^{\infty} \frac{d\delta^*}{d\xi}\frac{d\xi}{dS}\frac{d\xi}{x-\xi} \tag{4.10}$$

Then (4.9) becomes

$$\frac{U_e(x)}{U_0} = \left(\frac{x}{x + R_0/2}\right)^{\frac{1}{2}} \left[1 + \frac{1}{\pi}\int_0^{\infty} y_b'(\xi) \frac{d\xi}{x-\xi} + \frac{1}{\pi}\int_0^{\infty} \frac{d\delta^*}{d\xi}\frac{d\xi}{dS}\frac{d\xi}{x-\xi}\right]. \tag{4.11}$$

Lighthill's correction factor	primary flow field	Flow field generated by barrier itself	Boundary layer displacement effect

where R_0 radius of curvature of effective leading edge

$$R_0 = 8\,\epsilon_b^2 + \delta^*(0)$$

Near the blunt nose (4.11) indicates $U_e(x) \sim x^{1/2}$,

i.e., $U_e(s) \sim s$ and has the correct behavior by comparison with the exact solution of the potential-flow equation at stagnation region.

Combining (4.11), (3.19) and (3.20), we have three equations for three unknowns, which complete the formulation provided the boundary condition is properly given.

At the leading edge, the exact solution of two-dimensional stagnation flow gives the relation

$$\epsilon_v \, \delta^{*2} \frac{d U_e}{d x} \frac{d x}{d s} = 0.648^2 \qquad at \quad x = 0 \tag{4.12}$$

Sufficiently far downstream from the barrier, disturbances die out, and for the case of laminar, the boundary layer becomes of Blasius velocity profile.

Hence, $X >> 1$, $U_e = 1$, $H = H_b = 0.38414$ Laminar case (4.13)

Governing equation given by (4.12), (3.19), (3.20), (4.13) and boundary condition of (4.12) and (4.13) complete the present case of formulation.

IV.2 Case II: Stratified Flow Formulation

Two-dimensional stratified flow over a slender barrier in a semi-infinite domain are examined theoretically. The density gradient and ρU^2 are assumed to be constant upstream. Under these circumstances, governing equations could be reduced to a linear one, namely Helmholtz's equation (1). Although the governing equation is now the same as that of the diffraction theory, the boundary conditions are different, instead of Sommerfeld's radiation condition, solutions have to satisfy the condition of no waves far upstream,

as indicated by the experimental observation (6) (24).

For the present study, the classical technique of diffraction theory is used. A fundamental solution was first chosen, and the upstream waves were cancelled out with the aid of the remaining terms in the general solution. This technique has been used by Lyra (25) for the study of stationary lee waves of small amplitude over barriers with a uniform velocity and exponential density distribution upstream. Under the same assumption, Graham (26) applied this technique to stratified fluid flow over a slender body. For the case of a uniform upstream velocity and a uniform upstream density gradient, Pao (11) successfully applied this technique to solve problems by an inverse method, without assuming small amplitude wave motion.

In the following derivations, slender body assumption was used, but no assumption has been made on the amplitude of wave motion. The density gradient and ρU^2 are assumed to be constant upstream. Then the governing equations of two-dimensional, steady, incompressible, inviscid, stratified flows become

$$\nabla^2 \Delta + \sigma^2 \Delta = 0 \qquad (4.14)$$

Here $\sigma^2 \quad \frac{g}{U_o^2} \left| \frac{1}{\rho} \frac{d\rho}{dy_o} \right|$ is related to non-dimensional Richardson number Ri, based on the characteristic barrier height, by

$$\sigma^2 \epsilon_b^2 = \mathrm{Ri}, \text{ and } \Delta \equiv y_o - y, \qquad (4.15)$$

as in Figure (9), is the value of streamline displacement.

The general solution of equation (4.14) in polar co-ordinates is (Watson 1944)

$$\Delta = \sum_{n=1}^{\infty} \left[-a_n J_n(\sigma r) - b_n Y_n(\sigma r) \right] \left(C_n \cos n\theta + d_n \sin n\theta \right) \quad (4.16)$$

where $r = (x^2+y^2)^{1/2}$, $\theta = \tan^{-1}(y/x)$

In order to construct a doublet-like solution, the primary solution is chosen as $\Delta_p = -b_1 Y_1(\sigma r) \sin\theta$ (4.17)

For small r, $\Delta_p \sim \frac{1}{r} \sin\theta$ and behaves like a doublet in potential flow.

Then, from the remaining terms of equation (4.14), an auxiliary solution is sought which helps to cancel out the undesired disturbance of equation (4.17) at large distances upstream.

For large r, $Y_1(\sigma r) \cong \sqrt{\frac{2}{\pi\sigma r}} \sin\left(\sigma r - \frac{3\pi}{4}\right)$ (4.18)

$$J_n(\sigma r) \cong -\sqrt{\frac{2}{\pi\sigma r}} \sin\left(\sigma r - \frac{3\pi}{4} - \frac{n\pi}{2}\right) \quad (4.19)$$

For the function (4.28) to be in phase or 180° out of phase with the function (4.19), n must be an even number.

Thus, the auxiliary solution can be written as

$$\Delta_A = -\sum_{n=1}^{\infty} a_{2n} J_{2n}(\sigma r) \sin 2n\theta$$

The condition of cancelled upstream wave implies

$$\Delta = \Delta_A + \Delta_p = 0 \qquad r >> 1 \ , \quad \frac{\pi}{2} < \theta < \frac{3}{2}\pi \ ,$$

implies

$$-b_1 + \sum_{n=1}^{\infty} (-1)^n a_{2n} \sin 2n\theta = 0 \qquad \frac{\pi}{2} \le \theta \le \frac{3}{2}\pi$$

$$\therefore \quad a_n = \frac{b_1}{\pi} \frac{8n}{4n^2-1}$$

and $$\Delta = -b_1 Y_1(\sigma r)\sin\theta - \frac{b_1}{\pi}\sum_{n=1}^{\infty}\frac{8n}{4n^2-1}J_{2n}(\sigma r)\sin 2n\theta$$

$$\equiv -b_1\frac{2}{\sigma}K(x,y) \tag{4.20}$$

Thus (4.20) is the solution generated by a single doublet. For a doublet with strength b at $(\xi, 0)$, (4.20) becomes

$$\Delta = -\frac{2b}{\sigma}K(x-\xi, y) \tag{4.21}$$

Equation (4.21) can be integrated to obtain the flow field generated by a single source at ξ_1, as

$$\Delta = -\int_{\xi_1}^{\infty}\frac{2b}{\sigma}K(x-\xi, y)\,d\xi \tag{4.22}$$

By definition

$$u = -\frac{\partial\psi}{\partial y} = U(y_0)\frac{\partial y_0}{\partial y} = U(y_0)\left(1+\frac{\partial\Delta}{\partial y}\right)$$

$$v = \frac{\partial\psi}{\partial x} = -U(y_0)\frac{\partial y_0}{\partial x} = -U(y_0)\frac{\partial\Delta}{\partial x} \tag{4.23}$$

So that the $v(x, y)$ generated by a single source at ξ_1, is

$$v(x,y) = -U(y_0)\frac{\partial\Delta}{\partial x} = U(y_0)\frac{2b}{\sigma}\frac{\partial}{\partial x}\int_{\xi_1}^{\infty}K(x-\xi, y)\,d\xi$$

By the use of mathematical relations

$$\frac{\partial}{\partial x}\int_{\xi_1}^{\infty}f(x-\xi)\,d\xi = -\int_{\xi_1}^{\infty}\frac{\partial}{\partial\xi}f(x-\xi)\,d\xi = f(x-\xi_1)$$ the expression for v becomes

$$v(x,y) = U(y_0)\frac{2b}{\sigma}K(x-\xi_1, y) \tag{4.24}$$

For a continuous source distribution with strength $f(\xi)$ starting at origin,

$$v(x,y) = \frac{2}{\sigma}\int_0^{\infty}U(y_0)f(\xi)K(x-\xi, y)\,d\xi$$

As $y \to 0$, the contribution to the integral comes only from $\xi = x$ and also $U(y_0) \to U_0$

Therefore,

$$v(x,0^+) = \lim_{\substack{y\to 0^+ \\ \epsilon_3 \to 0}} U_0 y f(x) \int_{x-\epsilon_3}^{x+\epsilon_3} \frac{Y_1\left(\sigma\sqrt{y^2+(x-\xi)^2}\right)}{\sqrt{y^2+(x-\xi)^2}} d\xi$$

$$+ \lim_{\substack{y\to 0^+ \\ \epsilon_3 \to 0}} \frac{U_0 f(x)}{\pi} \sum_{n=1}^{\infty} \frac{8n}{4n^2-1} \int_{x-\epsilon_3}^{x+\epsilon_3} J_{2n}\left(\sigma\sqrt{y^2+(x-\xi)^2}\right) \sin\left(2n \tan^{-1}\frac{y}{x-\xi}\right) d\xi \qquad (4.25)$$

For small argument $\left(\sigma\sqrt{y^2+(x-\xi)^2}\right)$

$$Y_1\left(\sigma\sqrt{y^2+(x-\xi)^2}\right) \cong -2 \Big/ \left(\pi\sigma\sqrt{y^2+(x-\xi)^2}\right)$$

$$J_{2n}\left(\sigma\sqrt{y^2+(x-\xi)^2}\right) \cong \frac{1}{(2n)!}\left[\frac{\sigma\sqrt{y^2+(x-\xi)^2}}{2}\right]^{2n} \qquad (4.26)$$

So that (4.25) becomes,

$$V(x,0^+) = \lim_{\substack{y\to 0^+ \\ \epsilon_3 \to 0}} U_0 y f(x) \int_{x-\epsilon_3}^{x+\epsilon_3} \frac{-2\,d\xi}{\pi\sigma\left[y^2+(x-\xi)^2\right]} +$$

$$\sum_{n=1}^{\infty} \frac{8n}{\pi(4n^2-1)} \frac{f(x)}{(2n)!\,2^{2n}} \lim_{\substack{y\to 0^+ \\ \epsilon_3 \to 0}} \int_{x-\epsilon_3}^{x+\epsilon_3} \left[\alpha\sqrt{y^2+(x-\xi)^2}\right]^{2n} \sin\left(2n\tan^{-1}\frac{y}{x-\xi}\right) d\xi$$

$$= \lim_{\substack{y\to 0^+ \\ \epsilon_3 \to 0}} U_0 y f(x) \int_{x-\epsilon_3}^{x+\epsilon_3} \frac{-2d\xi}{\pi\sigma\left[y^2+(x-\xi)^2\right]} + \lim_{y\to 0^+} o(y)$$

$$= -\frac{2U_0 f(x)}{\sigma} \qquad (4.27)$$

The boundary condition for slender body is

$$\frac{V(\xi,0^+)}{U_0} = \frac{-2f(\xi)}{\sigma} = \tan\Theta = \frac{dy_e}{d\xi} \tag{4.28}$$

where y_e is the thickness of effective barrier.

$$\therefore \quad f(\xi) = -\frac{\sigma}{2}\frac{dy_e}{d\xi} \quad , \quad \frac{dy_e}{d\xi} = \frac{dy_b}{d\xi} + \frac{d\delta^*}{ds}$$

The source distribution required to produce a given body y_b (x) is thus defined.

Alternately, the dipole distribution, $g(\xi)$, can be obtained by integration $g(\xi) = \int_0^{\xi} f(\xi')\,d\xi' = -\frac{\sigma}{2} y_e(\xi)$

From (4.21) the flow field generated by the body y_e(x) is then given by

$$\Delta(x,y) = \int_0^{\infty} y_e(\xi)\, K(x-\xi, y)\, d\xi \tag{4.30}$$

From (4.23)

$$u = U(y_0)\left[1 + \frac{\partial \Delta}{\partial y}\right]$$

$$= U(y_0)\left[1 + \int_0^{\infty} y_e(\xi)\frac{\partial K(x-\xi,y)}{\partial y}\, d\xi\right] \tag{4.31}$$

from which surface speed "U_e" could be calculated.

The detail work is similar to the case of potential flow.

V. NUMERICAL ANALYSIS FOR INCOMPRESSIBLE SEPARATED FLOW

The problem of viscous-inviscid interaction at supersonic speed has been successfully treated in recent years. However, very few published examples of work appear for the case of low-speed flow. One of the reasons is that the case of low-speed flow is far more difficult; the governing equations are elliptic in nature in subsonic region, which requires that the interaction between the inviscid and the inner viscous layer is not local but global.

In these days, it appears that two possible mathematical techniques have been developed for obtaining a solution of low speed separated flow problem; namely, boundary-layer integral methods and finite difference methods for the full Navier-Stokes equations.

The boundary-layer integral analysis of Lees and Reeves (3) has demonstrated good agreement with experimental data in supersonic flow. Recently this method has been used for the case of subsonic and transonic flow problem by Alber (4) (23). This method considers flow field to be composed of two distinguishable viscous and inviscid fluid flow regions, keeps only essential global feature of each flow field, and it is relatively simple. But there remains a principal difficulty to be overcome; the development of a convergent iteration scheme which could properly match the boundary layer with the outer inviscid flow.

On the other hand, the time dependent numerical solution of full Navier-Stokes equation by Nakayama and Daly and Harlow (27, 28), finite difference form, certainly eliminates the problem of matching

but it is much more complicated and introduces different kinds of difficulties such as long computer times, question of numerical stability.

As already mentioned, the principal difficulty of applying Lees and Reeves integral theory to subsonic separated flow problem is the difficulty of developing a convergent iteration scheme which could properly match the boundary layer with the outer inviscid flow field. However, the recent computation of transonic flow by Klineberg and Steger (29), which includes the separated boundary layer flow along the surface and the wake downstream of the airfoil, shows that the iteration scheme they developed is a converging one.

In this section an iterative scheme following the Klineberg-Steger method is developed for calculating the incompressible flow field which includes the separated and reattached boundary-layer flow along the surface.

V. 1 The Basic Iteration Scheme

Starting with the given body shape, the corresponding inviscid flow field could be calculated by thin airfoil theory. The computed surface pressure (or surface speed)is then specified for the boundary layer calculation and the equations are integrated toward the separation point for obtaining the corresponding δ^*. At this location, the boundary layer equations have a singularity and the solution diverges. A joining point x_J is then selected upstream of this location. To continue the iteration sequence, the distribution of the $\tan\Theta$ is arbitrarily specified over the remaining part of the flow field ($x > x_J$). With the specified $\tan\Theta$, $\tan\Theta \equiv \frac{dy_b}{dx} + \frac{d\delta^*}{ds}$, the boundary layer

equations are integrated over the flowfield beyond the joining point, and the corresponding U_e distribution is computed.

Upstream of the joining point, with the computed δ^* distribution, we calculate the effective body shape $\bar{y}_e$. Then, with the effective body shape upstream of the joining point and the computed U distribution downstream of the joining point given, the inviscid flow field is calculated with the mixed boundary conditions. The solution of Laplace equation of potential flow with this mixed boundary condition provides corrected values for u and v in the regions upstream and downstream of the joining point, respectively. These distributions are then used as the input of the boundary-layer calculation in the respective regions and the alternate iteration of the inner and outer solution is continued until a desired convergence is achieved.

This scheme is illustrated in the sketch on the following page.

V.2 Inviscid Flow Calculation

Consider the case of symmetrical Joukowski airfoil connected with a semi-infinite flat plate downstream.

This body is given by,

$$\begin{aligned} y_b &= 0 && \text{for } x < 0 \\ y_b &= 4\epsilon_b x^{\frac{1}{2}}(1-x)^{\frac{3}{2}} && \text{for } 0 \le x \le 1 \\ y_b &= 0 && \text{for } 1 < x \end{aligned} \qquad (5.1)$$

The corresponding inviscid flow field is calculated by thin airfoil theory. The surface speed "U_e" is

$$"U_e" = 1 + \frac{1}{\pi}\int_{-\infty}^{\infty} \frac{y_b'(\xi)}{x-\xi} d\xi$$

Iteration Scheme

(1) With given body shape Calculate $u_e(x)$ from inviscid thin airfoil theory

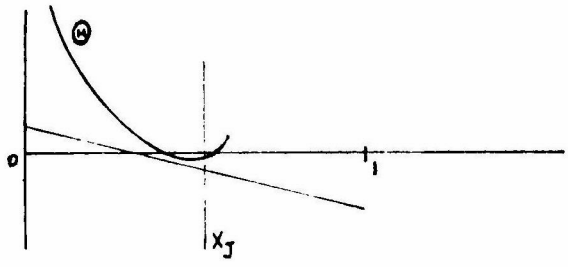

(2) With computed u_e, calculate Θ distribution from boundary layer equations

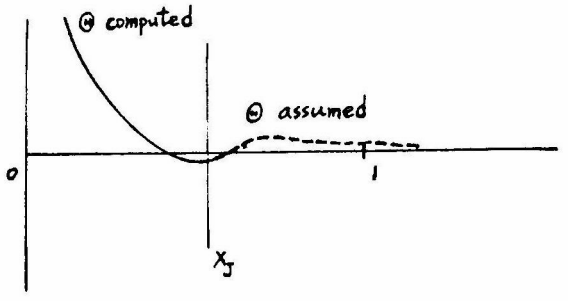

(3) Select a joining point x_J or s_J and assume a Θ distribution for $s > s_J$

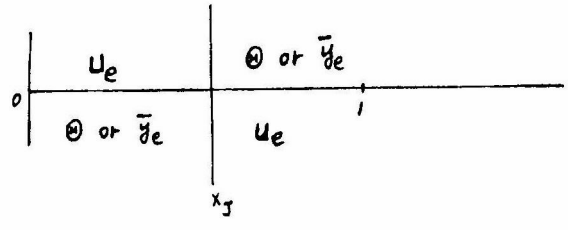

(4) Given u_e for $x \le x_J$
Θ for $x \ge x_J$
Calculate Θ for $x \le x_J$
u_e for $x \ge x_J$
From boundary layer equations

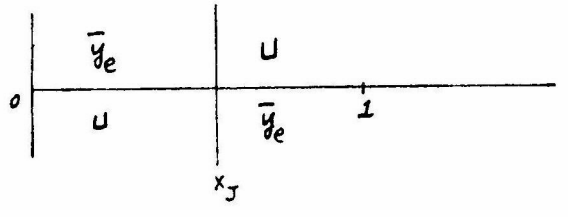

(5) Given computed $\bar{y}_e$ for $x \le x_j$
computed u for $x \ge x_j$
Compute u for $x \le x_j$
Compute $\bar{y}_e$ for $x \ge x_j$
from Laplace (inviscid) equations

(6) Go back to (4) if not converged

$$= \begin{cases} 1 + 2\,\epsilon_b\,(3-4x) & \text{for } 1 \geq x \geq 0 \\ 1 + 2\,\epsilon_b\left[(3-4x)+(4x^2-5x+1)(x^2-x)^{-\frac{1}{2}}\right] & \text{for } x > 1 \end{cases}$$

The uniformly valid expression of "U_e" is obtained after applying Lighthill's multiplicative correction for blunt nose body. Then

$$U_e(x) = \sqrt{\frac{x}{x+4\epsilon_b^2}} \begin{cases} 1+2\epsilon_b(3-4x) & \text{for } 1 \geq x \geq 0 \\ 1+2\epsilon_b\left[(3-4x)+(4x^2-5x+1)(x^2-x)^{-\frac{1}{2}}\right] & \text{for } x > 1 \end{cases} \quad (5.2)$$

where $4\epsilon_b^2$ is one half of the leading edge radius.

V.3 Forward Portion Boundary Layer Computation

The governing equations are

Momentum Integral Equation $$H\frac{d\delta^*}{ds} + \delta^*\frac{dH}{ds} + (2H+1)\frac{\delta^*}{U_e}\frac{dU_e}{ds} = \frac{\epsilon_v P}{U_e \delta^*} \quad (3.19)$$

Mechanical Energy Integral Equation

$$J\frac{d\delta^*}{ds} + \delta^*\frac{dJ}{ds} + 3J\,\frac{\delta^*}{U_e}\frac{dU_e}{ds} = \frac{\epsilon_v R}{U_e \delta^*} \quad (3.20)$$

where $\epsilon_v \equiv \nu / U_0 \ell$.

These are rewritten as

$$\begin{aligned} \frac{H}{2}\,\frac{d\delta^{*2}}{ds} + \delta^{*2}\frac{dH}{ds} + (2H+1)\frac{\delta^{*2}}{U_e}\frac{dU_e}{ds} &= \frac{\epsilon_v P}{U_e} \\ \frac{J}{2}\,\frac{d\delta^{*2}}{ds} + \delta^{*2}J'\frac{dH}{ds} + 3J\,\frac{\delta^{*2}}{U_e}\frac{dU_e}{ds} &= \frac{\epsilon_v R}{U_e} \end{aligned} \quad (5.3)$$

The initial conditions at the leading edge are obtained from the stagnation-point solution that is locally similar ($dH/ds = 0$) and $U_e \propto s$. This requirement provides relation for the initial profile quantities and displacement thickness.

$$3PJ - (1+2H)R = 0$$

$$\frac{1}{\epsilon_v}\delta^{*2}\frac{dU_e}{ds} = \frac{R}{3J} \tag{5.4}$$

The present curve fitting formulae for P, J, R give

$$H = 0.4499334$$

$$\delta^{*2} = 0.4214910\ \epsilon_v \Big/ \left(\frac{dU_e}{ds}\right) \qquad at \quad s = 0 \tag{5.5}$$

Eq. (5.3) with the specified U_e of (5.2) can be rewritten as

$$\frac{d\delta^{*2}}{ds} = \frac{2\epsilon_v\left\{(PJ'-R)+\left[3J-(2H+1)J'\right]\frac{\delta^{*2}}{\epsilon_v}\frac{dU_e}{ds}\right\}}{U_e(HJ'-J)}$$

$$\frac{dH}{ds} = \frac{\epsilon_v\left\{(RH-PJ)+J(1-H)\frac{\delta^{*2}}{\epsilon_v}\frac{dU_e}{ds}\right\}}{U_e\delta^{*2}(HJ'-J)} \tag{5.6}$$

Eq. (5.6) with initial condition (5.5) are solved by Runge-Kutta integration for $\delta^{*2}(s)$ and H(s).

It should be noted that, in the right hand sides of the expression (5.6), the denominators go to zero as U_e goes to zero at the leading edge. At the same place, by using the relation of (5.4), it can be shown that the numerators go to zero too. In order to approach the stagnation-point solution at the leading edge, the numerators should vanish faster than the denominator does. It can be shown by applying the l'Hospital rule that it is the case provided $\frac{d^2U_e}{ds^2} = 0$ at the leading edge, which is satisfied for the symmetric nose shapes. In the present computation, $U_e(x)$ is approximated by cubic spline, i.e., piecewise cubic polynominal with continuous first and second order derivative. In order to have $d^2U_e/ds^2 = 0$ at the leading edge, the natural spline is used.

Even with $U_e(s)$ satisfying the condition, the computation near the leading edge still needs more attention. The following series expansion was used for the computation near the leading edge.

For $s \ll 1$, Let

$$\begin{aligned} H &= H_0 + H_2 s^2 + \cdots \\ \delta^{*2} &= \delta_0 + \delta_2 s + \cdots \\ U_e &= U_1 + U_3 s^3 + \cdots \\ J &= J_0 + J_0' H_2 s^2 + \cdots \end{aligned} \tag{5.7}$$

etc.

After substituting (5.7) into (5.3) and equating like powers of s, we obtain

$s^{(0)}$

$$\begin{aligned} (1+2H_0)\,\delta_0 U_1 &= P_0 \epsilon_v \\ 3 J_0 \delta_0 U_1 &= R_0 \epsilon_v \end{aligned} \tag{5.8}$$

$s^{(2)}$

$$\begin{aligned} \left[(1+3H_0)U_1\right]\delta_2 + \left[4U_1\delta_0 - \epsilon_v P_0'\right] H_2 &= -3U_3(1+2H_0)\delta_0 \\ \left[4U_1 J_0\right]\delta_2 + \left[5U_1\delta_0 J_0' - \epsilon_v R_0'\right] H_2 &= -9U_3 J_0 \delta_0 \end{aligned} \tag{5.9}$$

Here (5.8), which gives the value of δ_0 and H_0 in terms of U_1, is equivalent to the initial condition (5.4).

δ_2 and H_2 are obtained from (5.9).

V.4 Boundary Layer Computation in Strong Interaction Region

The ordinary boundary-layer computation cannot proceed beyond the separation. Near this location, $(HJ' - J)$ goes to zero. The governing equation (5.6) is singular and the solution diverges.

The joining point was chosen at ten boundary-layer thicknesses upstream of this location. Downstream of the joining point $\tan\Theta$ distribution is assumed in the following form:

$$\tan\Theta(s) = \begin{cases} (as^2+bs+c)\,e^{-2s^2} & \text{for } s_1 \geq s \geq s_J \qquad (5.10) \\ 0.8617258\,\epsilon_v^{\frac{1}{2}}/(s-a_0)^{1/2} & \text{for } s \geq s_1 \qquad (5.11) \end{cases}$$

where s_J is the value of s corresponding to the joining point. a, b and c are constants calculated from the matching conditions of $\tan\Theta(s_J)$ $d\tan\Theta(s_J)/ds$, $d^2\tan(s_J)/ds^2$ between previously calculated and the form given in (5.10).

$\tan\Theta(s)$ in (5.11), which corresponds to the correct asymptotic behavior, i.e., constant velocity Blasius solution, is then matched to $\tan\Theta(s)$ given in (5.10). By requiring the continuity of $\tan\Theta$ and $\frac{d}{ds}\tan\Theta$, the position of matching, s_1, and the effective origin, a_0, are computed.

With the assumed $\tan\Theta$, $(\tan\Theta = d\delta^*/ds + d\eta_b/dx)$, $\frac{d\delta^*}{ds}$ for $s \geq s_J$ are known. Approximating $d\delta^*/ds$ by spline and integrating it by the Simpson's rule, the δ^* distribution was obtained.

With the specified $\delta^*(s)$, the boundary-layer equation (5.3) can be rewritten as follows.

$$\frac{dH}{ds} = \frac{\frac{\epsilon_v}{U_e}\left[3JP-(2H+1)R\right]+\frac{J}{2}(1-H)\frac{d\delta^{*2}}{ds}}{\delta^{*2}\left[3J-J'(2H+1)\right]}$$

$$\frac{dU_e}{ds} = \frac{\epsilon_v\left[R-PJ'\right]+\frac{U_e}{2}(HJ'-J)\frac{d\delta^{*2}}{ds}}{\delta^{*2}\left[3J-J'(2H+1)\right]} \qquad (5.12)$$

With the initial condition $H(s_J)$, $U_e(s_J)$ specified from the previous computation, (5.12) could then be integrated.

In the present computation, the computation is carried out to the point at ten times body chord length from the origin. After

this point the behavior of U_e could be obtained by asymptotical analysis. In order to match the U_e to its asymptotic form, the computation must be carried out at least to the point where $dU_e/ds > 0$.

V.5 Downstream Asymptotic Behavior of U_e

Because the subsonic separated flow problem is an elliptic one, the interaction is global, and the proper treatment of the downstream asymptotic behavior is then crucial for the convergence of the whole iteration scheme.

At large distances downstream from the body, the classical boundary-layer concept is then applicable; namely U_e can be calculated simply from the inviscid theory. Furthermore, in this region the disturbance generated by the body and the boundary-layer displacement effect could be approximated by a point force singularity acting near the origin. From the Blasius' law in two-dimensional potential flow, it follows immediately that an axial force corresponds to a source. Hence,

$$U_e = 1 + \frac{a}{x+b} \quad \text{for } y = 0, \quad x \gg 1 \tag{5.13}$$

Here a, b are constant, and are computed by matching U_e and dU_e/dx at the farthest grid point of the boundary-layer computation.

V.6 Inviscid Flow Computation - The Mixed Boundary Value Problem

From the previous boundary-layer computation, $\bar{y}_e$ and u are obtained for $s \leq s_J$ and $s \geq s_J$, respectively. With this computed v and u, say $v = g(x)$, $u = f(x)$, the inviscid flow field is calculated as follows.

First of all, the governing equation, the Laplace equation is linear. Then, the superposition principle could be used to decompose the present problem to two simple ones, the first problem and the

second problem.

The first problem is a conventional one: with the specified $v(x)$ for $x \leq x_J$ and a suitably chosen $v(x)$, say $v(x) = \hat{g}(x)^*$ for $x > x_J$ as boundary condition. The corresponding velocity u can be calculated from the thin airfoil theory. Call the computed u as $u_1(x)$.

The second problem is then a mixed boundary-value one: given the boundary condition, $v(x) = 0$ for $x \leq x_J$ and $u(x) = f(x) - u_1(x)$ for $x \geq x_J$, then compute $u(x)$ and $v(x)$ for $x \geq x_J$ and $x \leq x_J$, respectively, say $u = u_2(x)$, $v = v_2(x)$.

The superposition could be expressed as follows:

		x_J	
Prob. 1	Given	$v = g(x)$	$v = \hat{g}(x)$
	Obtained	$u = u_1(x)$	
Prob. 2	Given	$v = o$	$u = f(x) - u_1(x) \equiv f_2(x)$
	Obtained	$u = u_2(x)$	$v = v_2(x)$
Prob. 1 + Prob. 2	Obtained	$v = g(x)$ "u" $= u_1(x) + u_2(x)$	$u = f(x)$ $v = \hat{g}(x) + v_2(x)$

V.7 The First Problem

Given $v = g(x)$ for $x \leq x_J$ and $v = \hat{g}(x)$ for $x \geq x_J$, $u_1(x)$ can be calculated by the thin airfoil theory.

---

* In principle $\hat{g}(x) \equiv 0$ may be used. In practice, however, a form for $\hat{g}(x)$ is chosen such that $v(x)$ is smooth at $x = x_J$ in order to avoid the singularity in the corresponding $u(x)$ distribution.

$$u_1(x) = 1 + \frac{1}{\pi}\int_0^{\infty} \frac{v(\xi)}{x-\xi}\,d\xi$$

$$= 1 + \frac{1}{\pi}\left\{ \int_0^{x_J} \frac{g(\xi)\,d\xi}{x-\xi} + \int_{x_J}^{\infty} \frac{\hat{g}(\xi)\,d\xi}{x-\xi} \right\} \qquad (5.14)$$

where $g(\xi)$ was approximated by

$$g(\xi) = v_j + \frac{v_{j+1} - v_j}{x_{j+1} - x_j}(\xi - x_j) \qquad \text{for } x_{j+1} \geq \xi \geq x_j$$

$$j = 2, 3, \cdots (M_4 - 1) \qquad (5.15)$$

where $x(M_4) \equiv x_J$.

$$g(\xi) \equiv v_b'(\xi) + \frac{d\delta^*}{ds}(\xi)$$

$$= 2\epsilon_b x^{-\frac{1}{2}} + \epsilon_b\left(\frac{4\delta_2}{\delta_0^{1/2}} - 9\right)x^{\frac{1}{2}} + \left(\frac{15}{4}\epsilon_b + \frac{2}{3}a_1\frac{\delta_2}{\delta_0^{1/2}}\right)x^{\frac{3}{2}}$$

$$\text{for } x_2 > \xi > 0 \qquad (5.16)$$

where $a_1 \equiv (1 - 36\epsilon_b^2)/4\epsilon_b$.

$$\hat{g}(\xi) = \frac{g_1}{\xi} + \frac{g_2}{\xi^2} \qquad (5.17)$$

where g_1, g_2 are constant, obtained from the condition $g(x_J) = \hat{g}(x_J)$ and $g'(x_J) = \hat{g}'(x_J)$.

With the expression of $g(\xi)$ and $\hat{g}(\xi)$ given above the integration of (5.14) is carried out analytically. During the summation process terms with logarithmic singularities at the end points of the subintervals cancel each other.

V.8 The Problem 2

The problem 2 is solved by means of the technique of complex variables. By the symmetry property, the problem in the semi-infinite domain ($y \geq 0$) is extended to the problem in the whole xy plane with a straight line cut ($x \geq x_J$, $y = 0$). The boundary condition in this plane is: $u = f_2(x)$ on $(x > x_J, y = \pm 0)$.

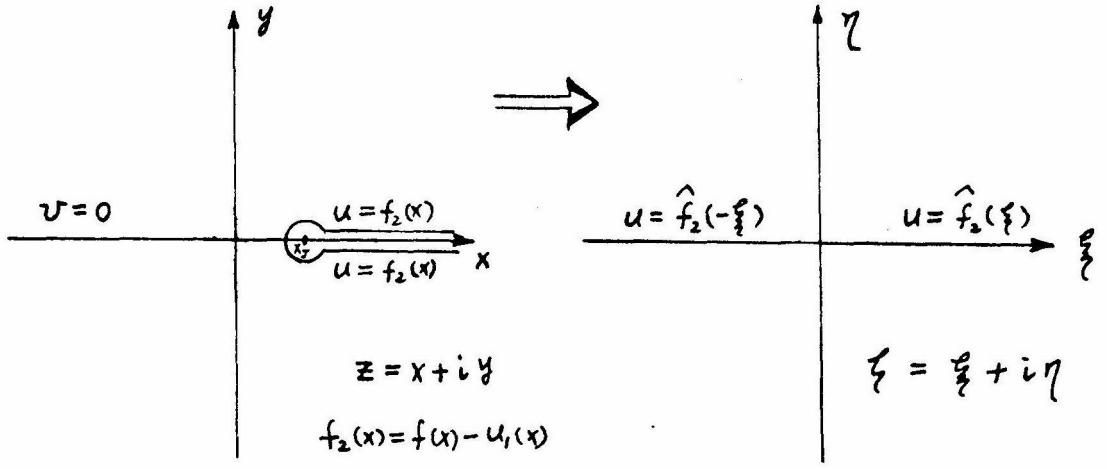

By using the transformation $\zeta = (z - x_J)^{1/2}$, the boundary $(x > x_J, y = \pm 0)$ is mapped on the $\eta = 0$ axis in ζ - plane.

By mapping the complex velocity at the corresponding points, the boundary condition on $\eta = 0$ becomes

$$u = f_2(\xi(x)) = \hat{f}_2(\xi)$$

From the symmetry it is obvious that

$$\hat{f}_2(-\xi) = \hat{f}_2(\xi)$$

The complex velocity $W(\zeta) = u - iv = \frac{i}{2\pi} \int_{-\infty}^{\infty} \frac{\varphi(\xi')\, d\xi'}{\zeta - \xi'}$

$$= \frac{i}{2\pi} \int_{-\infty}^{\infty} \frac{\varphi(\xi')[(\xi - \xi') - i\eta]}{(\xi - \xi')^2 + \eta^2} d\xi'$$

So that

$$u(\xi,\eta)=\frac{1}{2\pi}\int_{-\infty}^{\infty} q(\xi')\,\frac{\eta}{(\xi-\xi')^2+\eta^2}\,d\xi' \tag{5.18}$$

$$v(\xi,\eta)=\frac{-1}{2\pi}\int_{-\infty}^{\infty} q(\xi')\,\frac{\xi-\xi'}{(\xi-\xi')^2+\eta^2}\,d\xi' \tag{5.19}$$

From (5.18)

$$q(\xi)=\begin{cases} 2\hat{f}_2(\xi) & 0<\xi<\infty \\ 2\hat{f}_2(-\xi) & -\infty<\xi<0 \end{cases}$$

Thus

$$u(\xi,\eta)=\frac{1}{\pi}\int_0^{\infty}\hat{f}_2(\xi')\left[\frac{\eta}{(\xi-\xi')^2+\eta^2}+\frac{\eta}{(\xi+\xi')^2+\eta^2}\right]d\xi'$$

$$v(\xi,\eta)=-\frac{1}{\pi}\int_0^{\infty}\hat{f}_2(\xi')\left[\frac{\xi-\xi'}{(\xi-\xi')^2+\eta^2}-\frac{\xi+\xi'}{(\xi+\xi')^2+\eta^2}\right]d\xi'$$

From $\zeta=(z-x_J)^{1/2}$ it follows that

$$\xi^2-\eta^2=x-x_J \qquad \text{and} \qquad 2\xi\eta=y$$

Hence

$$\xi^2=\frac{1}{2}\left[\sqrt{(x-x_J)^2+y^2}+(x-x_J)\right]$$

$$\eta^2=\frac{1}{2}\left[\sqrt{(x-x_J)^2+y^2}-(x-x_J)\right]$$

On $y=0$, $x>x_J$ we have $\xi^2=x-x_J$, $\eta^2=0$

$y=0$, $x<x_J$ we have $\xi^2=0$, $\eta^2=-(x-x_J)$

Hence

$$u_2(x<x_J,\,y=0)=\frac{2}{\pi}\int_0^{\infty}\hat{f}_2(\xi')\,\frac{\sqrt{-(x-x_J)}}{\xi'^2-(x-x_J)}\,d\xi'$$

$$v_2\,(x>x_J,\ y=0) = \frac{2}{\pi}\int_0^\infty \hat{f}_2(\xi')\frac{\sqrt{x-x_J}}{\xi'^2-(x-x_J)}\,d\xi' \qquad (5.20)$$

Let $\xi' = (x'-x_J)^{1/2}$ then $\xi'^2 = x'-x_J$ and $d\xi' = dx'/2\sqrt{x'-x_J}$

Furthermore $\hat{f}_2(\xi') = f_2[x(\xi')] = f_2(x')$ by definition.

Therefore (5.20) becomes

$$u_2(x) = \frac{1}{\pi}(x_J-x)^{\frac{1}{2}}\int_0^\infty \frac{f_2(x')\,dx'}{(x'-x)(x'-x_J)^{1/2}} \quad \text{for } x < x_J$$

$$v_2(x) = \frac{1}{\pi}(x-x_J)^{\frac{1}{2}}\int_0^\infty \frac{f_2(x')\,dx'}{(x'-x)(x'-x_J)^{1/2}} \quad \text{for } x > x_J \qquad (5.21)$$

In computing the integral of (5.21) from $x' = o$ to $x' = x_M$, where x_M is the farthest computed point, the approach similar to that used in computing u_1 was used. $f_2(x')$ was approximate by continuous line segment from each grid point to the next one. Then the integration was carried out exactly. During the summation process, terms with singular behavior cancel out each other.

V.9 Downstream Asymptotical Analysis of Inviscid Computation

In order to carry out the integral of (5.21) from $x' = x_M$ to $x' \to \infty$, it is necessary to have the correct asymptotical expression of $f_2(x')$, i.e. $f(x') - f_1(x')$. The asymptotical behavior of $f(x)$, i.e. $u_e(x)$ in the boundary layer computation, was obtained in (V.5). The asymptotic behavior of u_1 is obtained by examining the expression of u_1

$$u_1(x) = 1 + \frac{1}{\pi}\int_0^\infty \frac{v(\xi)\,d\xi}{x-\xi}$$

$$= 1 + \frac{1}{\pi}\left\{\int_0^{x_J}\frac{v(\xi)\,d\xi}{x-\xi} + \int_{x_J}^\infty \frac{\frac{q_1}{\xi}+\frac{q_2}{\xi^2}}{x-\xi}\,d\xi\right\}$$

$$u_1(x) = 1 + \frac{1}{\pi}\left\{ \int_0^{x_J} \frac{v(\xi)\,d\xi}{x-\xi} + \frac{g_2}{x\,x_J} + \left(\frac{g_1}{x} + \frac{g_2}{x^2}\right) \log\left|\frac{x-x_J}{x_J}\right| \right\}$$

For $x >> x_J$

$$\int_0^{x_J} \frac{v(\xi)}{x-\xi}\,d\xi = \frac{1}{x}\int_0^{x_J} v(\xi)\,d\xi + O\left(\left(\frac{x_J}{x}\right)^2\right) = O\left(v_J \cdot \frac{x_J}{x}\right)$$

$$\frac{g_2}{x\,x_J} = \frac{g_2}{x_J^2}\,\frac{x_J}{x} = O\left(v_J \cdot \frac{x_J}{x}\right)$$

$$\frac{g_1}{x} + \frac{g_2}{x^2} = \frac{g_1}{x_J}\,\frac{x_J}{x} + \frac{g_2}{x_J^2}\,\frac{x_J^2}{x^2} = O\left(v_J \cdot \frac{x_J}{x}\right)$$

$$\bar{g}_2 \equiv g_2 + x_J \int_0^{x_J} v(\xi)\,d\xi$$

Hence for $x >> 1$ we obtain

$$u_1(x) \doteq 1 + \frac{1}{\pi}\left\{ \frac{\bar{g}_2}{x\,x_J} + \left(\frac{g_1}{x} + \frac{g_2}{x^2}\right) \log\left|\frac{x-x_J}{x_J}\right| \right\}$$

and $f_2(x) \equiv f(x) - u_1(x)$

$$= \frac{a}{x+b} - \frac{1}{\pi}\left\{ \frac{\bar{g}_2}{x\,x_J} + \left(\frac{g_1}{x} + \frac{g_2}{x^2}\right) \log\left|\frac{x-x_J}{x_J}\right| \right\}$$

Then the integral of (5.21) could be calculated exactly from $x' = x_M$ to $x' \to \infty$. The result is:

$$\int_{x_M}^{\infty} \frac{f(x') - u_1(x')\;dx'}{(x'-x)(x'-x_J)^{1/2}} = \int_{x_M}^{\infty} \frac{\frac{a}{x'+b} - \frac{1}{\pi}\left[\frac{\bar{g}_2}{x'x_J} + \left(\frac{g_1}{x'} + \frac{g_2}{x'^2}\right)\log\left|\frac{x'-x_J}{x_J}\right|\right]}{(x'-x)(x'-x_J)^{1/2}}\,dx'$$

$$= \left(\frac{a}{b+x}\right) \begin{cases} \text{if } (x_J+b)>0 & \left\{\frac{-2}{(x_J+b)^{1/2}}\right\} \operatorname{ctn}^{-1}\left(\frac{x_M-x_J}{x_J+b}\right)^{1/2} \\ \text{if } (x_J+b)<0 & \left\{\frac{-1}{[-(x_J+b)]^{1/2}}\right\} \log\left|\frac{[-(x_J+b)]^{1/2}+(x_M-x_J)^{1/2}}{[-(x_J+b)]^{1/2}-(x_M-x_J)^{1/2}}\right| \\ \text{if } (x_J+b)=0 & -2(x_M-x_J)^{-1/2} \end{cases}$$

$$+ \left\{\frac{a}{b+x} - \frac{\bar{g}_2}{\pi x x_J} + \left(\frac{g_1}{\pi x}+\frac{g_2}{\pi x^2}\right)\log x_J\right\} \begin{cases} \text{if } (x_J-x)>0 & \frac{2}{(x_J-x)^{1/2}} \operatorname{ctn}^{-1}\left(\frac{x_M-x_J}{x_J-x}\right)^{1/2} \\ \text{if } (x_J-x)<0 & \frac{-1}{[-(x_J-x)]^{1/2}} \log\left|\frac{[-(x_J-x)]^{1/2}+[x_M-x_J]^{1/2}}{[-(x_J-x)]^{1/2}-[x_M-x_J]^{1/2}}\right| \\ \text{if } (x_J-x)=0 & 2(x_M-x_J)^{-\frac{1}{2}} \end{cases}$$

$$+ \left\{-\frac{\bar{g}_2}{\pi x_J} + \left(\frac{g_1}{\pi}+\frac{g_2}{\pi x}\right)\log x_J\right\}\left(-\frac{2}{x x_J^{1/2}}\right) \operatorname{ctn}^{-1}\left(\frac{x_M-x_J}{x_J}\right)$$

$$+ \left\{\frac{4}{x}\left(\frac{g_1}{\pi}+\frac{g_2}{\pi x}\right) + \frac{2g_2}{\pi x x_J}\right\} \frac{1}{x_J^{1/2}} \left\{\left[\log(x_M-x_J)^{1/2}\right] \operatorname{ctn}^{-1}\left(\frac{x_M-x_J}{x_J}\right)^{1/2}\right.$$

$$\left. + \left(\frac{x_J}{x_M-x_J}\right)^{1/2} - \frac{1}{3^2}\left(\frac{x_J}{x_M-x_J}\right)^{3/2} + \frac{1}{5^2}\left(\frac{x_J}{x_M-x_J}\right)^{5/2} - \cdots \right\}$$

$$+\left\{-\frac{g_1}{\pi}-\frac{g_2}{\pi x}\right\}\left(\frac{4}{x}\right)\begin{cases}\text{if } (x_J-x)>0 & \left\{\frac{1}{(x_J-x)^{1/2}}\right\}\left\{\left[\log(x_M-x_J)^{1/2}\right]\text{ctn}^{-1}\left(\frac{x_M-x_J}{x_J-x}\right)^{1/2}\right. \\ & \left.+\left(\frac{x_J-x}{x_M-x_J}\right)^{1/2}-\frac{1}{3^2}\left(\frac{x_J-x}{x_M-x_J}\right)^{3/2}+\frac{1}{5^2}\left(\frac{x_J-x}{x_M-x_J}\right)^{5/2}-\cdots\right\} \\ \text{if } (x_J-x)<0 & \left\{\frac{1}{(x-x_J)^{1/2}}\right\}\left\{\left[\log(x_M-x_J)^{1/2}\right]\text{ctn}^{-1}\left(\frac{x_M-x_J}{x_J-x}\right)^{1/2}\right. \\ & \left.+\left(\frac{x-x_J}{x_M-x_J}\right)^{1/2}+\frac{1}{3^2}\left(\frac{x-x_J}{x_M-x_J}\right)^{3/2}+\frac{1}{5^2}\left(\frac{x-x_J}{x_M-x_J}\right)^{5/2}+\cdots\right\} \\ \text{if } (x_J-x)=0 & \left\{\frac{\log(x_M-x_J)^{1/2}}{(x_M-x_J)^{1/2}}+\frac{1}{(x_M-x_J)^{1/2}}\right\}\end{cases}$$

$$+\left(\frac{g_2}{\pi x}\right)\left\{2\left[-\frac{(x_M-x_J)^{1/2}\log(x_M-x_J)^{1/2}}{x_M x_J}-\frac{1}{x_J^{3/2}}\text{ctn}^{-1}\left(\frac{x_M-x_J}{x_J}\right)^{1/2}\right]+\frac{(x_M-x_J)^{1/2}\log x_J}{x_M x_J}\right.$$

$$\left.-\frac{1}{x_J^{3/2}}(\log x_J)\,\text{ctn}^{-1}\left(\frac{x_M-x_J}{x_J}\right)^{1/2}\right\} \qquad (5.22)$$

Although Eq. (5.22) is correct from a mathematical point of view, it is not a suitable form for numerical computation for small values of x. A recombination of various terms give the following form for $x < x_J$,

$$\int_{x_M}^{\infty} \frac{f(x') - u_1(x')}{(x'-x)(x'-x_J)^{1/2}}\,dx' \qquad \text{for} \quad x < x_J$$

$$= \left(\frac{a}{b+x}\right)\left\{\begin{array}{ll} \text{if } (x_J+b)>0 & \left\{\frac{-2}{(x_J+b)^{1/2}}\right\} \operatorname{ctn}^{-1}\left(\frac{x_M-x_J}{x_J+b}\right)^{1/2} \\ \text{if } (x_J+b)<0 & \left\{\frac{-1}{[-(x_J+b)]^{1/2}}\right\} \log\left|\frac{[-(x_J+b)]^{1/2}+(x_M-x_J)^{1/2}}{[-(x_J+b)]^{1/2}-(x_M-x_J)^{1/2}}\right| \\ \text{if } (x_J+b)=0 & -2(x_M-x_J)^{-\frac{1}{2}} \end{array}\right\}$$

$$+ \frac{2}{(x_J-x)^{1/2}} \frac{a}{b+x} \operatorname{ctn}^{-1}\left(\frac{x_M-x_J}{x_J-x}\right)^{1/2} + \frac{4}{\pi} \frac{1}{(x_M-x_J)^{3/2}} \left\{ -\frac{1}{3}\left[g_1\left(\frac{1}{2}\log\left|\frac{x_M-x_J}{x_J}\right| + \frac{1}{3}\right)\right.\right.$$

$$\left. + \frac{g_2}{2x_J}\right] + \sum_{N=2}^{\infty}\left[\frac{(-1)^{N+1}}{2N+1}\left(\frac{x_J}{x_M-x_J}\right)^{N-1}\left\{\left[g_1\left(\frac{1}{2}\log\left|\frac{x_M-x_J}{x_J}\right| + \frac{1}{2N+1}\right) + \frac{g_2}{2x_J}\right]\left[\sum_{j=1}^{N} {}_NC_j (-1)^j (\right.\right.\right.$$

$$\left.\left.\left. -1)^j \left(\frac{x}{x_J}\right)^{j-1}\right] + \frac{g_2}{x_J}\left[\frac{1}{2}\log\left|\frac{x_M-x_J}{x_J}\right| + \frac{1}{2N+1}\right]\left[\sum_{j=2}^{N} {}_NC_j (-1)^j \left(\frac{x}{x_J}\right)^{j-2}\right]\right\}\right]$$

$$\left. + \frac{\hat{g}_2}{2} x_J^{N-1} \sum_{j=1}^{N} {}_NC_j (-1)^j \left(\frac{x}{x_J}\right)^{j-1}\right\}$$

where $\quad {}_NC_j \equiv \dfrac{N!}{j!\,(N-j)!}$

$$\hat{g}_2 \equiv x_J \int_0^{x_J} U(\xi)\,d\xi$$

V. 10 Solution of Mixed Boundary Problem

From (5.21) and (V.6), the solution of the complete mixed boundary problem with $v = g(x)$ for $x \leq x_J$, $u = f(x)$ for $x \geq x_J$ given, turns out to be

$$\begin{aligned} u(x) &= u_1(x) + u_2(x) \qquad \text{for} \quad x < x_J \\ v(x) &= g(x) + v_2(x) \qquad \text{for} \quad x > x_J \end{aligned} \tag{5.23}$$

where $$u_1(x) = 1 + \frac{1}{\pi}\left\{ \int_0^{x_J} \frac{g(\xi)\,d\xi}{x-\xi} + \int_{x_J}^{\infty} \frac{\hat{g}(\xi)\,d\xi}{x-\xi} \right\} \qquad \text{for all } x$$

$$\hat{g}(x) = \frac{g_1}{x} + \frac{g_2}{x^2} \qquad \text{for } x \geq x_J$$

$$u_2(x) = \frac{1}{\pi}(x_J - x)^{\frac{1}{2}} \int_0^{\infty} \frac{f(\xi) - u_1(\xi)}{(\xi - x)(\xi - x_J)^{1/2}}\,d\xi \qquad \text{for } x < x_J$$

$$v_2(x) = \frac{1}{\pi}(x - x_J)^{\frac{1}{2}} \int_0^{\infty} \frac{f(\xi) - u_1(\xi)}{(\xi - x)(\xi - x_J)}\,d\xi \qquad \text{for } x > x_J$$

The "u(x)" of (5.23) was then corrected to be a uniformly valid solution by multiplying by the Lighthill's correction factor, which in this case, equals

$$L = \left(\frac{\pi}{\pi + 4\epsilon_b^2} \right)^{\frac{1}{2}}$$

So that

$$u(x) = L\left[u_1(x) + u_2(x)\right] \qquad \text{for} \quad x < x_J$$

$$v(x) = \hat{q}(x) + v_2(x) \qquad \text{for} \quad x > x_J \qquad (5.24)$$

V.11 The Completed Iteration

With the computed u(x) for $x < x_J$ and $\tan\Theta$ for $x > x_J$, $\tan\Theta \equiv V(x)$, the boundary-layer equations can then be integrated as described in (V.3,4).

VI. CONCLUSIONS

In the present study, the complete integral formulation of both inner and outer flow field of stratified flow over a barrier was obtained. Furthermore, an iteration scheme of computation is proposed for the simpler case of incompressible homogeneous flow over a barrier with viscous-inviscid interaction included.

It is believed that with the completed basic formulation and proposed computation scheme mentioned above, the gross effect of boundary layer separation on the stratified flow field could be estimated by means of the integral method of Lees and Reeves.

REFERENCES

1. Long, R. R.: "Some Aspects of the Flow of Stratified Fluids - I. A Theoretical Investigation," Tellus, A Quarterly Journal of Geophysics, Vol. 5, No. 1, pp. 42-58, May 1953.
2. Davis, R. E.: "The Two-Dimensional Flow of a Stratified Fluid over an Obstacle," J. Fluid Mech., Vol. 36, Part I, pp. 127-143, 1969.
3. Reeves, B. L. and Lees, L.: "Theory of Laminar Near Wake of Blunt Bodies in Hypersonic Flow," AIAA Journal, Vol. 3, No. 11, pp. 2061-2074, Nov. 1965.
4. Alber, I. E.: "Integral Theory for Turbulent Base Flows at Subsonic and Supersonic Speeds," Ph. D. Thesis, California Institute of Technology, June 1967.
5. Grange, J. M., Klineberg, J. M., and Lees, L.: "Laminar Boundary-Layer Separation and Near Wake Flow for a Smooth Blunt Body at Supersonic and Hypersonic Speeds," AIAA Journal, Vol. 5, No. 6, pp. 1096-1098, June 1967.
6. Long, R. R.: "Some Aspects of the Flow of Stratified Fluids. II. Experiments with a Two-Fluid System," Tellus, Vol. 6, No. 2, pp. 97-115, May 1954.
7. Long, R. R.: "Some Aspects of the Flow of Stratified Fluids. III. Continuous Density Gradients," Tellus, Vol. 7, No. 3, pp. 341-356, 1955.
8. Pao, Y. H.: "Origin and Structure of Turbulence in Stably Stratified Media," Proceedings of a Symposium on Clear Air Turbulence and It's Detection held in Seattle, Washington, pp. 73-99, August 1968.
9. Pao, Y. H.: "Laminar, Transition and Turbulent Flows of Stably Stratified Fluids Over Barriers," Boeing Scientific Research Laboratories Document TM55, July 1968.
10. Pao, Y. H.: "Turbulence Measurements in Stably Stratified Fluids" Boeing Document D1-82-0959, Feb. 1970.
11. Pao, Y. H.: "Inviscid Flows of Stably Stratified Fluids Over Barriers," Quarterly Journal of the Royal Meteorological Society, Vol. 95, No. 403, pp. 104-119, Jan. 1969.
12. Debler, W. R.: "Stratified Flow Into a Line Sink," J. Eng. Mech., Div., Proc. ASCE, 85, pp. 51-65, 1959.
13. Yih, C. S.: "Effect of Density Variation on Fluid Flow," Journal of Geophysical Research, Vol. 64, pp. 2219-2223.
14. Trustrum, K.: "Rotating and Stratified Fluid Flow," Journal of Fluid Mech., Vol. 19, pp. 415, 1964.
15. Bretherton, F.: "The Time Dependent Motion Due to a Cylinder Moving in an Unbounded Rotating or Stratified Fluid," Journal of Fluid Mech., Vol. 28, pp. 545, 1967.

16. Kao, T. W.: "The Phenomenon of Blocking in Stratified Flows," J. Geophysical Research," Vol. 70, No. 4, pp. 815-822, 1965.

17. Alber, I. E. and Lees, L.: "Integral Theory for Supersonic Turbulent Base Flows," AIAA Journal, Vol. 6, No. 7, pp. 1343-1351, July 1968.

18. Stewartson, K.: "Further Solutions of the Falkner-Skan Equations," Proc. Cambridge Phil. Soc., 50, pp. 454-465, 1954.

19. Van Dyke, M.: "Higher Approximations in Boundary Layer Theory. Part 1: General Analysis," J. Fluid Mech., Vol. 14, pp. 481-495.

20. So, M. C. and Mellor, G. L.: "An Experimental Investigation of Turbulent Boundary Layers Along Curved Surfaces," NASA CR-140, April 1972.

21. Pao, Y. H., Callahan, M. E. and Timm, G. K.: "Vortex Streets in Stably Stratified Fluids," Boeing Document D1-82-0736, July 1968.

22. Alber, I. E.: "Similar Solutions for a Family of Separated Turbulent Boundary Layers," presented at AIAA 9th Aerospace Sciences Meeting, New York, N. Y., Jan. 25-27, 1971.

23. Alber, I. E., Bacon, J. W., Masson, B. S. and Collins, D.J.: "An Experimental Investigation of Turbulent Transonic Viscous-Inviscid Interactions," presented at AIAA 9th Fluid and Plasma Dynamics Conference, Palo Alto, California, June 21-23, 1971.

24. Pao, Y. H.: "Laminar Flow of a Stably Stratified Fluid Past a Flat Plate," J. Fluid Mech., Vol. 34, Part 4, pp. 795-808, 1968.

25. Lyra, G.: "Theory of Stationary Lee Waves in Free Atmosphere," Boeing Scientific Research Laboratories, Translation No. 409.

26. Graham, E. W.: "The Two-Dimensional Flow of an Inviscid Density-Stratified Liquid Past a Slender Body," Boeing Document D1-82-0550.

27. Nakayama, P. I.: "Turbulence Transport Equations and Their Numerical Solution," AIAA Paper No. 70-3.AIAA, 8th Aerospace Sciences Meeting, January 1970.

28. Daly, B.J. and Harlow, F.H.; "Inclusion of Turbulence Effect in Numerical Fluid Dynamics," Presented at 2nd International Conference on Numerical Methods in Fluid Dynamics. UC Berkeley Sept. 1970.

29. Klineberg, J. and Joseph Steger,: "Calculation of Separated Flows at Subsonic and Transonic Speeds," Presented at the Third International Conference on Numerical Methods in Fluid Dynamics, Paris, July 1972.

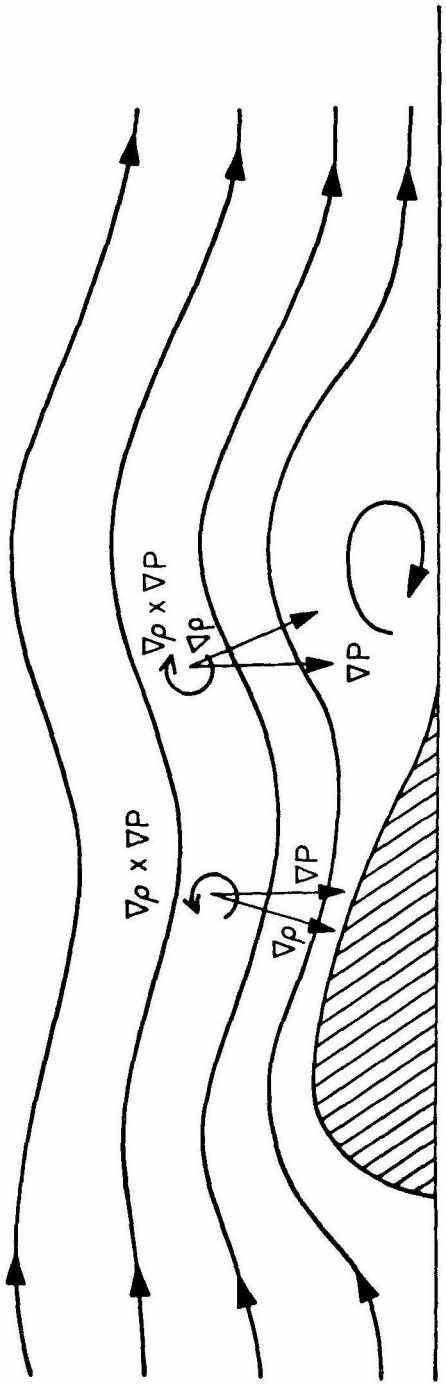

Fig. 1 Generation of lee waves.

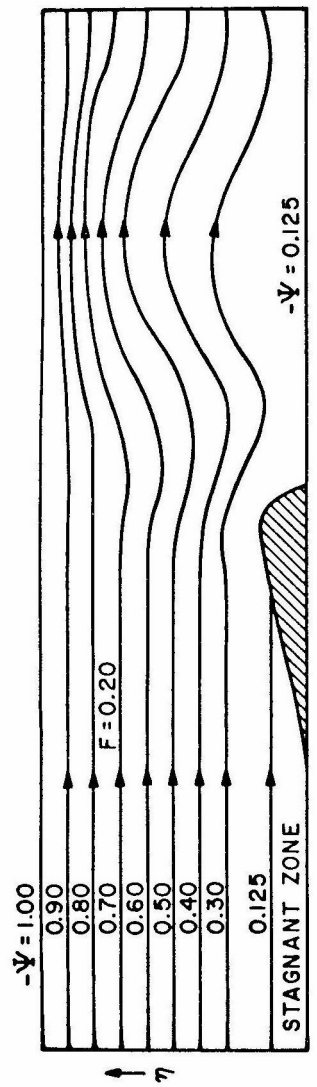

Fig. 2a Flow pattern over a wedge with stagnant zone in front of wedge, at Froude number equal to 0.20, or Ri ≈ 0.74.

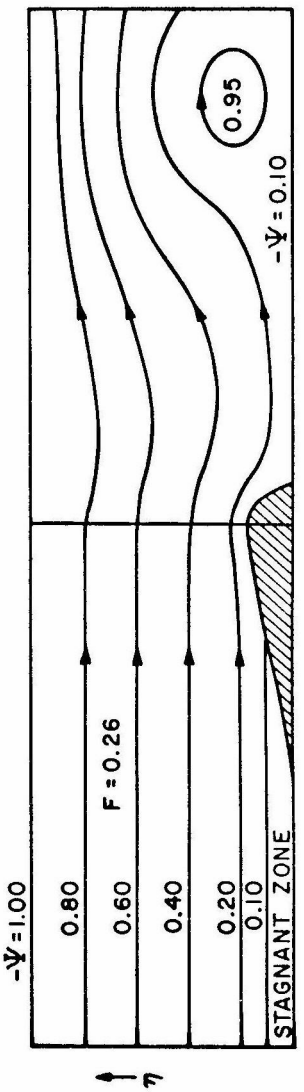

Fig. 2b Flow pattern over a wedge with stagnant zone in front of wedge, at Froude number equal to 0.25, or Ri ≈ 0.47.

Fig. 2 The phenomenon of blocking, follows Kao's calculation (16).

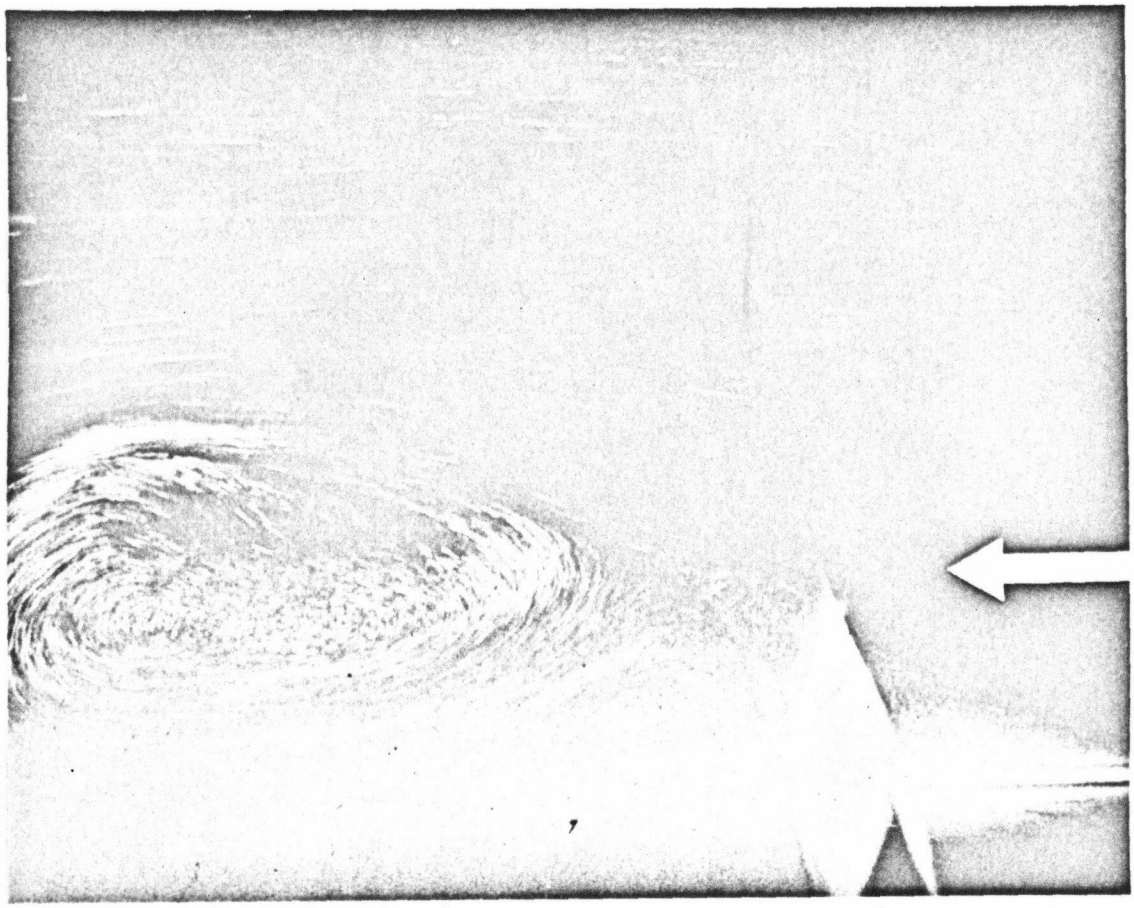

Fig. 3 The turbulent rotor by Pao(8).

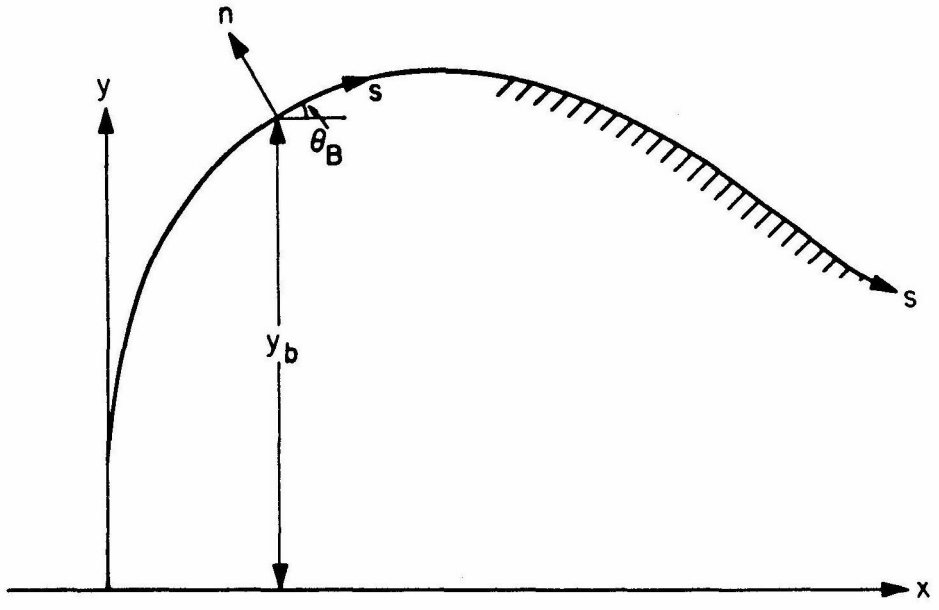

Fig. 4 Curvilinear co-ordinate system.

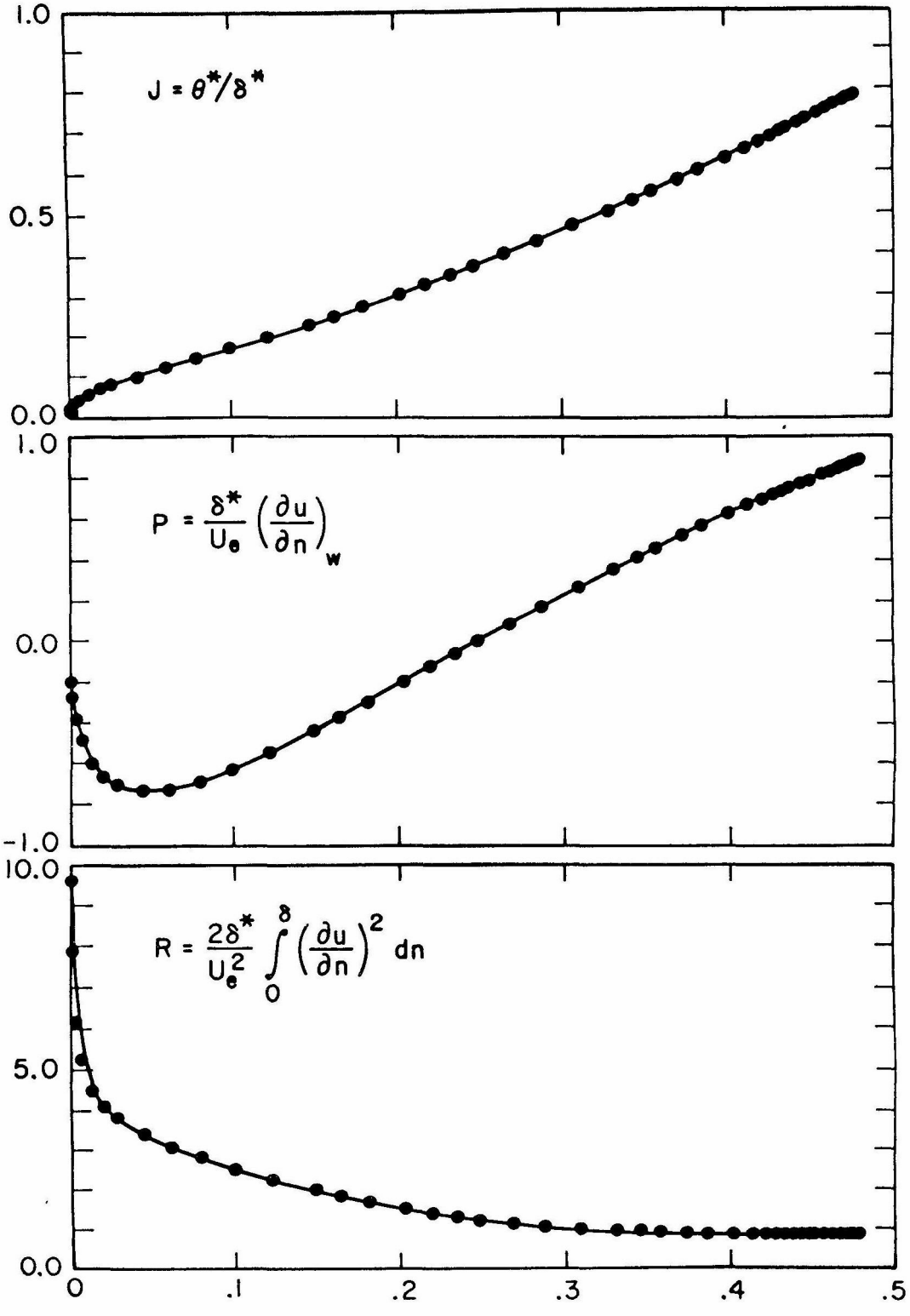
1.0
0.5
0.0
$J = \theta^*/\delta^*$
1.0
0.0
-1.0
$P = \frac{\delta^*}{U_e}\left(\frac{\partial u}{\partial n}\right)_w$
10.0
5.0
0.0
$R = \frac{2\delta^*}{U_e^2}\int_0^\delta \left(\frac{\partial u}{\partial n}\right)^2 dn$
0
.1
.2
.3
.4
.5

Fig. 5 J(H), P(H), R(H).

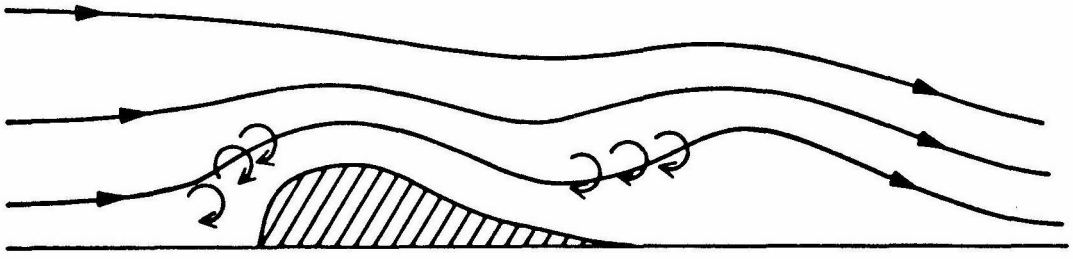

Fig. 6 Free stream vorticity generated by density stratification.

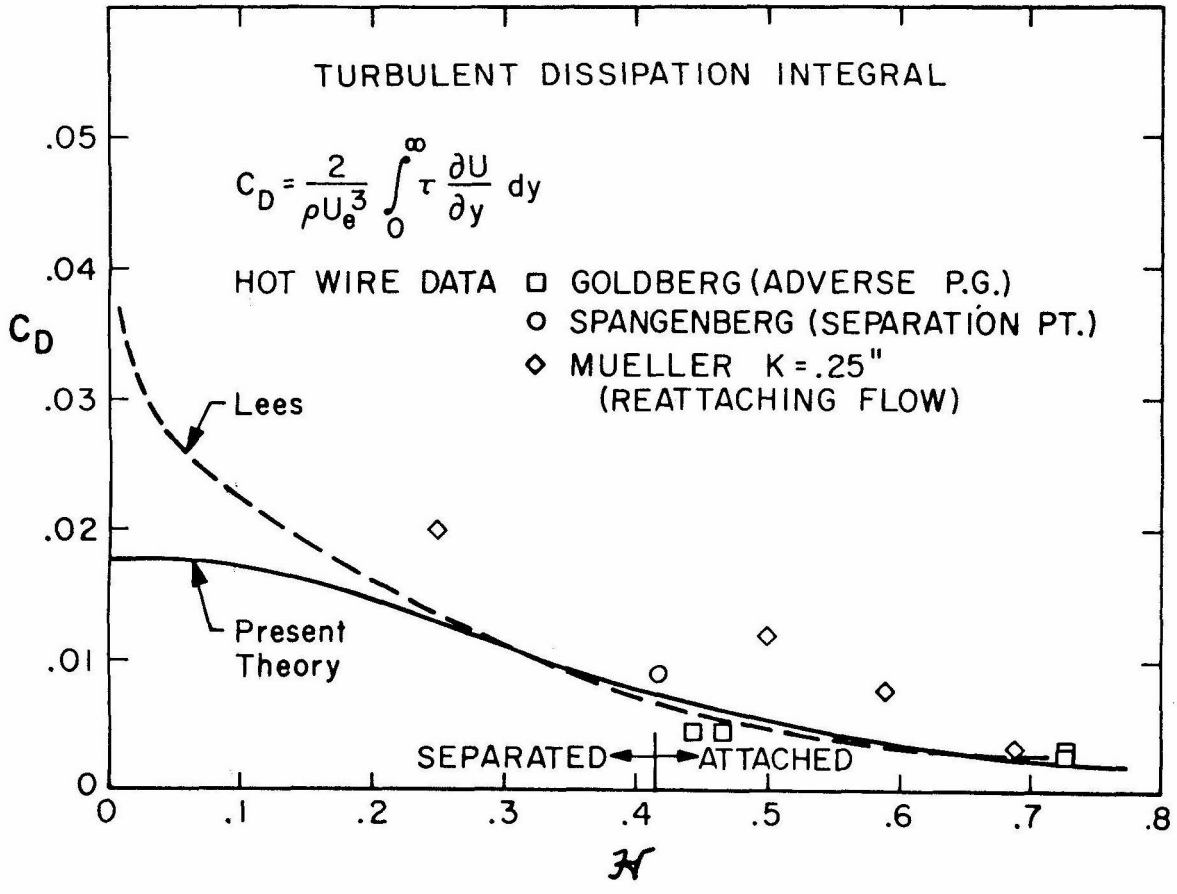

Fig. 7a $C_D(\mathcal{H})$ given by Alber (22,23).

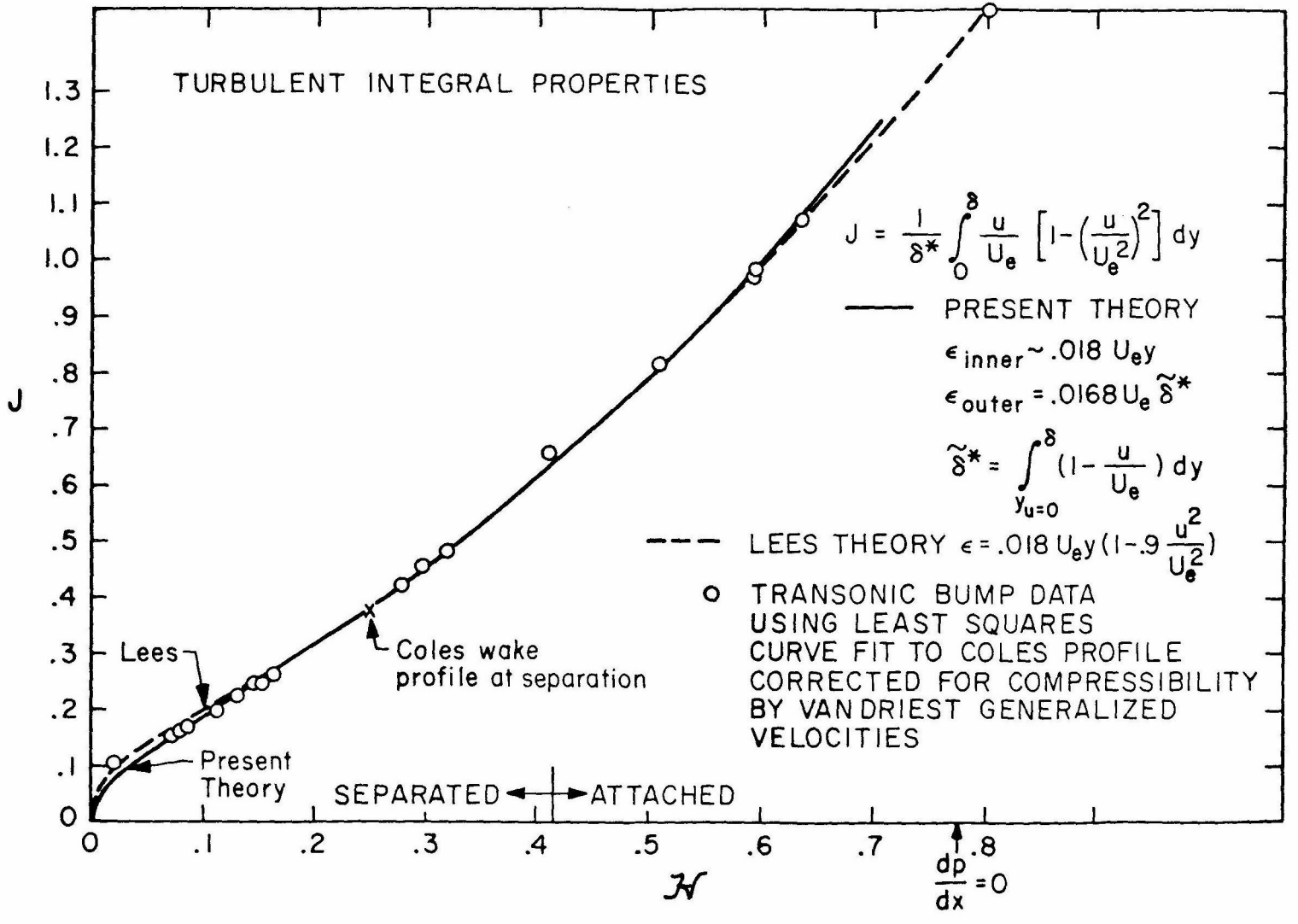

Fig. 7b $J_K(\mathcal{H})$ given by Alber (22, 23).

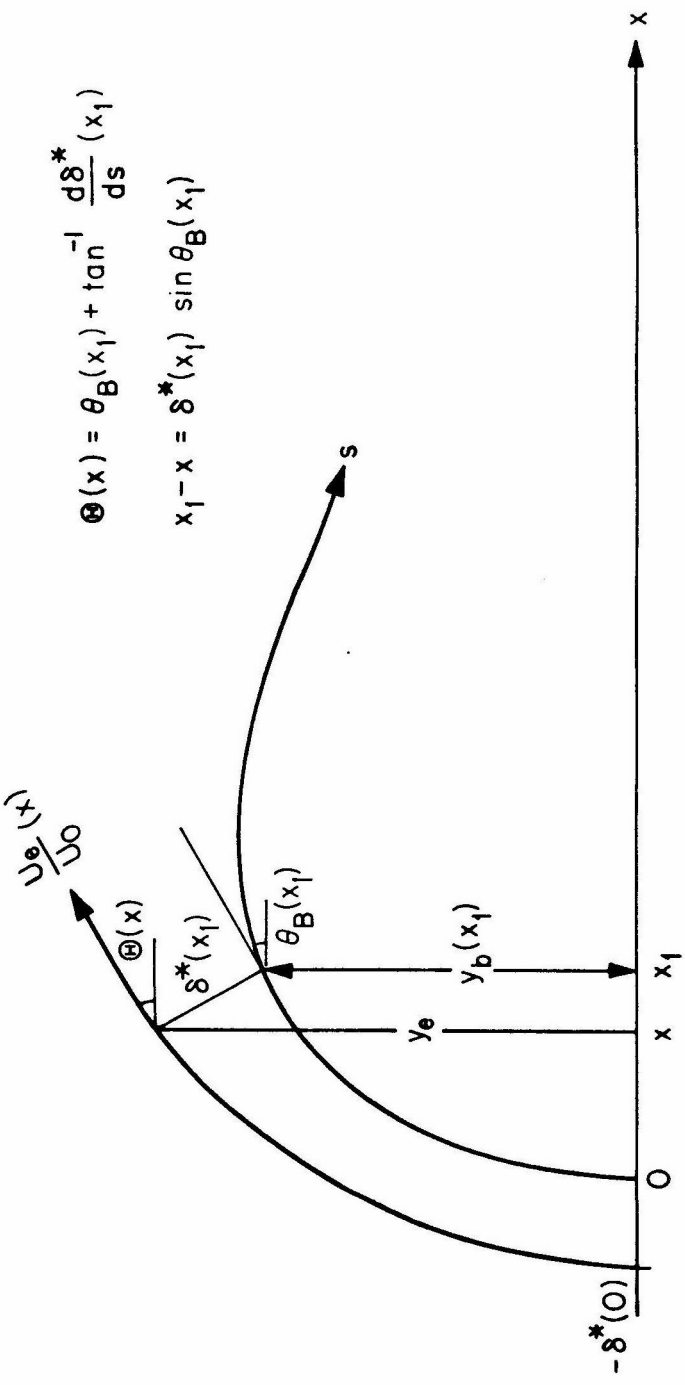

Fig. 8 Inviscid flow region.

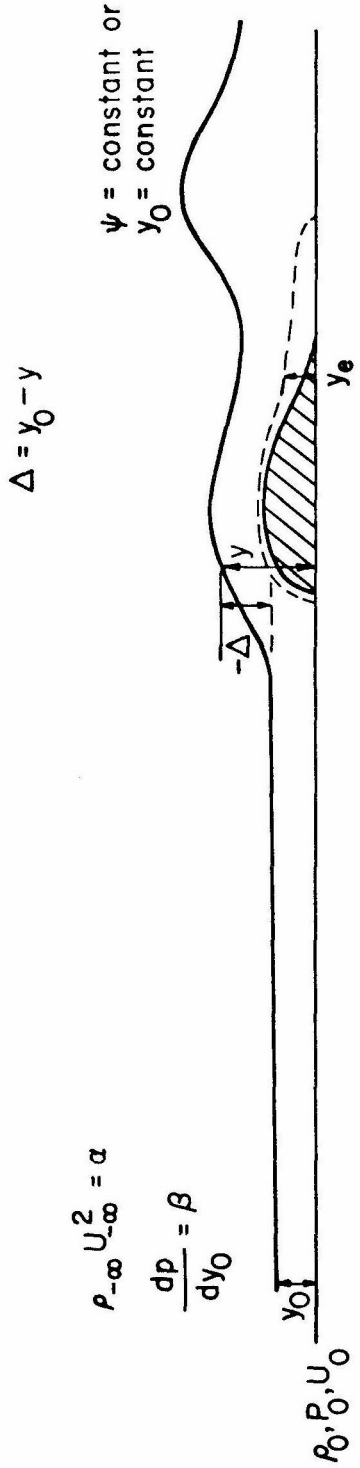

Fig.9 Inviscid outer flow field of stratified fluids over barriers.